Investigating the role of mitoNEET in iron overload-induced insulin resistance

Eddie Tam

A thesis submitted to the Faculty of Graduate Studies in partial fulfillment of the requirements for the degree of Master of Science

Graduate Program in Biology
York University, Toronto, Ontario
July 2023

ABSTRACT

Excess iron, in a process termed iron overload (IO) is closely linked to cardiovascular and metabolic diseases. Previous research has already established a causal link between IO and insulin resistance in both cardiac and skeletal muscle setting. Building upon this knowledge, the potential for mitoNEET to offer protection against IO-induced insulin resistance was investigated. The potential mechanisms underlying the protective effects of mitoNEET, which included mitochondrial dynamics, oxidative stress, and mitophagy, was also examined in H9c2 cardiac and L6 skeletal muscle cells. Using various experimental approaches including quantitative polymerase chain reaction (qPCR), western blot, fluorescent microscopy, and reporter cell lines, mitoNEET was shown to be protective against IO-induced insulin resistance. In H9c2 cells, mitoNEET provided protection by regulating mitochondrial iron and reactive oxygen species (ROS) to prevent insulin resistance. In L6 cells, mitoNEET prevented insulin resistance via regulation of mitochondrial iron, ROS, and mitochondrial fission.

ACKNOWLEDGMENTS

I would like to extend my gratitude to Dr. Gary Sweeney for the opportunity to complete my MSc under his supervision and guidance. I would like to thank members of the Sweeney lab for their support with special thanks to Dr. Hyekyoung (Cindy) Sung for serving an advisory role. I would also like to thank Dr. Kubiseski for his feedback regarding my research progress and presiding over my thesis defence. Finally, I would like to thank members of the examining committee, Dr. Christopher Perry, and Dr. Emanuel Rosonina, for taking time out of their busy schedule to examine my thesis.

ABBREVIATIONS

Akt ___ protein kinase B
BNIP3___ BCL2/adenovirus E1B 19 kDa protein-interacting protein 3
DMT1 ___ divalent metal transporter 1
Drp1 ___ dynamin related protein 1
ERK1/2 ___ extracellular signal-regulated protein kinase 1/2
EV ___ empty vector
FAS ___ ferric ammonium sulphate, $NH_4Fe(SO_4)_2$ FUNDC1___
FUN 14 domain containing 1
Grb2 ___ growth factor receptor-bound protein 2
IRE ___ iron response element
IRP ___ iron regulatory protein
IRS ___ insulin receptor substrate
IO ___ iron overload
MEK ___ mitogen-activated protein kinase kinase
MFF ___ MitoFerroFluor
Mt ___ Mitochondrial
Mtff___mitochondrial fission factor
Mfn1/2 ___ mitofusin1/2
MitoN ___ mitoNEET
mTORC2 ___ mammalian target of rapamycin complex 2
Opa1 ___ optic atrophy 1
PDK ___ 3-phosphoinositide-dependent protein kinase
PI3K ___ phosphatidylinositol (3,4,5)-triphosphate kinase
PINK1___ PTEN-induced kinase1
PIP2 ___ phosphatidylinositol 4,5-bisphosphate
PIP3 ___ phosphatidylinositol (3,4,5)-triphosphate
ROS ___ reactive oxygen species
SOS ___ son of sevenless
STEAP3 ___ six-transmembrane epithelial antigen of prostate 3
T2D ___ type 2 diabetes
Tf ___ tranferrin
TfR ___ transferrin receptor
TSAT___transferrin saturation

Table of Contents

1 CHAPTER 1: LITERATURE REVIEW

1.1 Iron metabolism

Iron is required for living things to carry out physiological processes, acting primarily as a cofactor in the form of a prosthetic group called iron sulfur clusters (ISCs). ISC-containing proteins play key roles in catalyzing metabolic reactions, mediating signaling pathways, and the regulation of iron homeostasis. Specific examples of processes that require ISCs include DNA replication and repair, cellular respiration, and cell cycle regulation [1,2].

Although iron is an essential nutrient for biological processes, there are mechanisms in place to ensure it is tightly regulated. Intracellular iron homeostasis is established by a balance between import, export, storage, and utilization. Import of extracellular iron, which is often found it the ferric form and bound to transferrin (Tf), is transported to transferrin receptor 1 (TfR1) [3]. Cells then import this iron through endocytosis into endosomes, where STEAP3 converts iron from the ferric state to the ferrous form [3]. DMT1 then transports ferrous iron out of endosomes and into the cytosol forming the labile iron pool [3]. This metabolically active form of iron can then be utilized for cellular processes as described above. Within the cell, mitochondria are a major source of iron utilization, however, the precise mechanism which iron is imported has not been fully characterized [3]. Intracellular iron is exported exclusively by ferroportins, a transmembrane transporter [4].

One way for regulating excess iron utilizes translational regulation from IRPs, which bind to specific untranslated regions of mRNA, IREs [1]. One such protein under the regulation of IRPs and IREs is ferritin which sequesters iron for storage [1]. When levels of iron are low, IRP binds to the IRE of ferritin mRNA at the 5’ end resulting in translational inhibition [1]. In response to too much iron, such as with IO, the IRP inhibition is relieved, thus increasing ferritin expression [2]. However, when ferritin becomes oversaturated by iron, it forms aggregates, and eventually gets degraded by lysosomes in a process termed ferritinophagy [5].

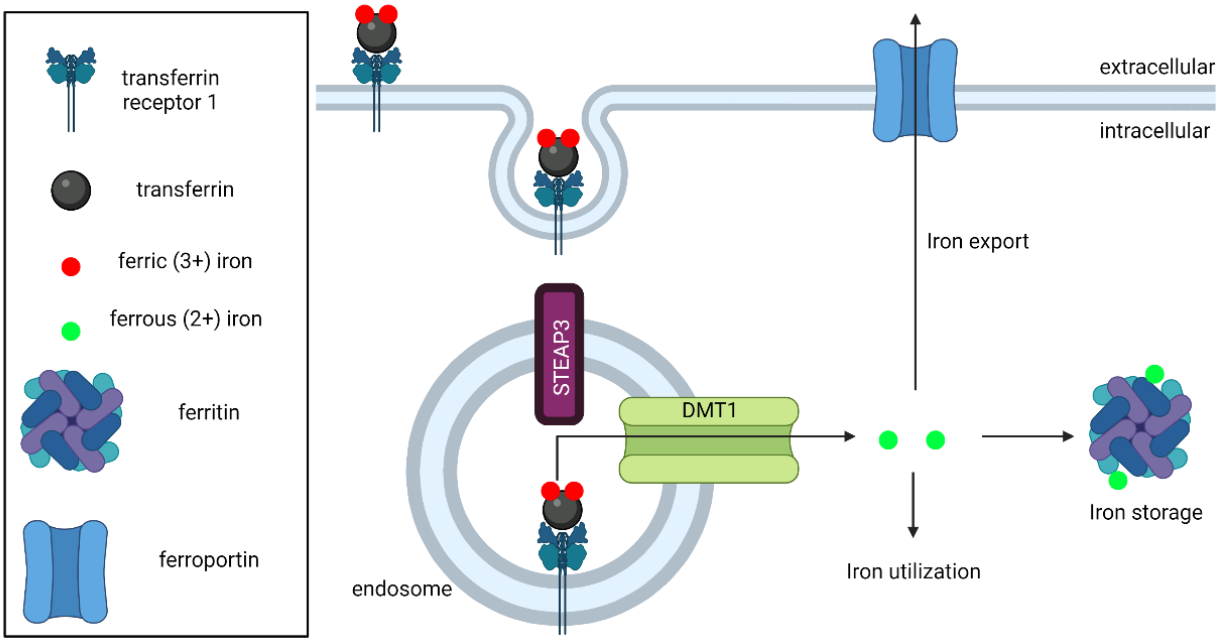

Figure 1. Schematic diagram of iron import, export, and storage. Extracellular iron, bound to transferrin in its ferric form, is imported into cells by transferrin receptor 1 – mediated endocytosis. In endosomes, iron is reduced to its ferrous form by STEAP3 and DMT1, then exported out of endosomes. Iron can then be utilized by the cell, stored in ferritin, or exported via ferroportins.

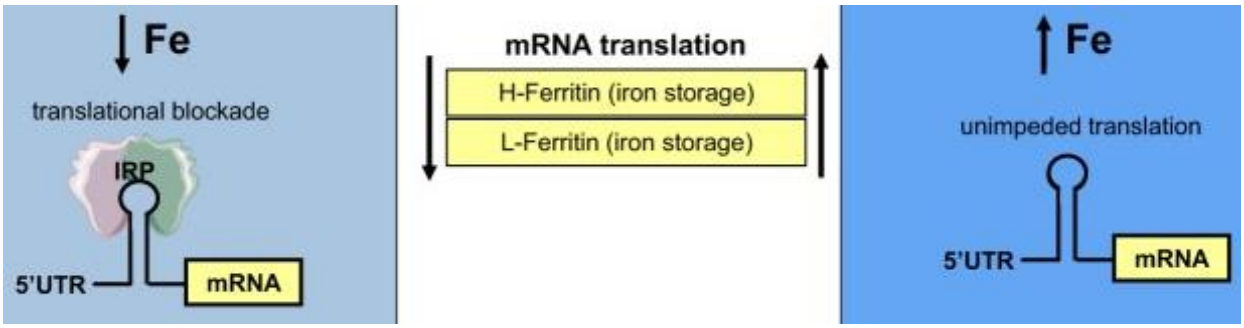

Figure 2. Mechanism of ferritin regulation. Ferritin mRNA is translationally repressed by iron regulatory protein (IRP) binding of the 5'UTR in a basal state as shown on the left. Increasing levels of iron (right) relieves the IRP repression allowing for increase in translation of ferritin mRNA [6].

1.2 Iron overload in clinical setting

Despite its importance, an excess of iron, termed iron overload (IO), has been linked to pathological conditions in humans such as metabolic syndrome and heart disease [7,8]. In a clinical setting, iron overload is defined as a surplus of iron stored in the body, notably in the liver, heart, and skeletal muscle. The gold standard for assessment of IO is to obtain a tissue biopsy to quantify the amount of stainable iron [9]. However, this method is highly invasive and much more costly than a blood tests. IO can be routinely diagnosed using blood tests such as serum transferrin saturation (TSAT), or serum ferritin levels. Normal range for transferrin saturation is 20% - 40%. Iron deficiency is diagnosed when TSAT falls below 20% and IO is diagnosed when TSAT exceeds 40%. However, the deleterious effects are not very apparent until TSAT levels surpass 60%-70% [10]. The normal range for serum ferritin in men is 30-300ng/mL and 10-200ng/mL in women [11]. Even though a serum ferritin and TSAT test only serve as an indirect indicator of iron levels, it remains a highly cost-effective and non-invasive method as an initial screen which continues to be applicable for clinical use [12].

Physiological concentration of serum iron in humans are estimated to be between 10µM and 30µM [13]. Total iron binding capacity can range up to 80µM, so the body can handle a mild excess in iron. Furthermore, serum iron concentration up to 89.5µM has demonstrated to have mild to no toxicity in humans. Adverse effects are more apparent once serum iron concentrations exceed 89.5µM and are particularly pronounced in concentrations above 179µM [14].

Iron overload can be classified as primary, or secondary. The underlying cause of primary IO is mutation in genes, such as HFE. The mostly widely studied mutation, is C282Y in the HFE protein which regulates the production of hepcidin, a key hormone involved in the negative regulation of iron import [15]. Secondary iron overload occurs as a result of increased iron intake through dietary means or blood transfusions. Nonetheless, IO, whether primary or secondary, has been linked to the development of diabetes and cardiovascular diseases [16]. One potential mechanism underlying the deleterious effects of IO is the induction of reactive oxygen species (ROS) [17,18].

1.3 Iron overload and oxidative stress

ROS are molecules derived from molecular oxygen that have undergone reaction to yield more toxic forms. Some common examples of ROS include hydroxyl radicals, hydrogen peroxides, and superoxides [17]. ROS is produced at low levels under physiological settings where it acts as signaling molecules that contribute to cell survival and proliferation. Physiological ROS originates from several subcellular components such as endoplasmic reticulum, peroxisomes, and mitochondria. It is generally accepted that mitochondria are the major source of ROS [17]. When the levels of ROS become elevated, several endogenous mechanisms are in place to re-establish homeostasis. Antioxidant mechanisms such as superoxide dismutase, glutathione peroxidase, and catalase are in place to prevent an excess production of ROS. Superoxide dismutase catalyzes the conversion of superoxide into oxygen and hydrogen peroxide, a less toxic form of ROS. Catalase further breaks down hydrogen peroxide into water and oxygen. Glutathione peroxidase catalyzes the reaction between glutathione and hydrogen

peroxide resulting in the breakdown into water. There are also non-enzymatic antioxidants such as NAD+/NADH and glutathione which can act as a buffer to compensate for mild redox imbalances through donation/acceptance of hydrogen and electrons. Despite these antioxidant mechanisms, pathological levels of ROS upregulation can exceed the endogenous antioxidant capacity resulting in disease. Specifically, under IO, the excess ROS generated can overwhelm these antioxidant mechanisms ultimately causing oxidative stress [19]. Oxidative stress has been linked with several pathologies such as insulin resistance, diabetes, and heart disease [19].

1.4 Insulin signaling and insulin resistance

Insulin is a peptide hormone that regulates several biological processes such as glucose, lipid, and energy metabolism [20]. Insulin exert many of its effects via activation of the Akt or ERK1/2 pathway [20].

In the Akt pathway, insulin binds to insulin receptors causing a conformational change and autophosphorylation at tyrosine residues. Phosphorylated insulin receptors recruit the adaptor protein, IRS, to be phosphorylated at tyrosine residues. Phosphorylated IRS allows for the recruitment and binding of SH2 domain containing molecules such as PI3K, which results in its activation. PI3K then phosphorylates PIP_2 to PIP_3, which recruits PDK-1 and mTORC2 to activate Akt via phosphorylation at threonine308 and serine473, respectively. Activated Akt regulates different genes responsible for metabolism, translation, and cell growth.

In the ERK1/2 pathway, Grb2 binds to IRS independently of PI3K. Grb2 allows for SOS to bind, which catalyzes the conversion of Ras-GDP to Ras-GTP. GTP bound Ras

then transduces its signal to Raf, which activates MEK1/2, resulting in phosphorylation and activation of ERK1/2. Like Akt, ERK1/2 also regulates genes for cell growth and proliferation [20]. Insulin resistance, which contributes to a broader condition called metabolic syndrome, occurs when there is an impairment in the insulin signaling pathway.

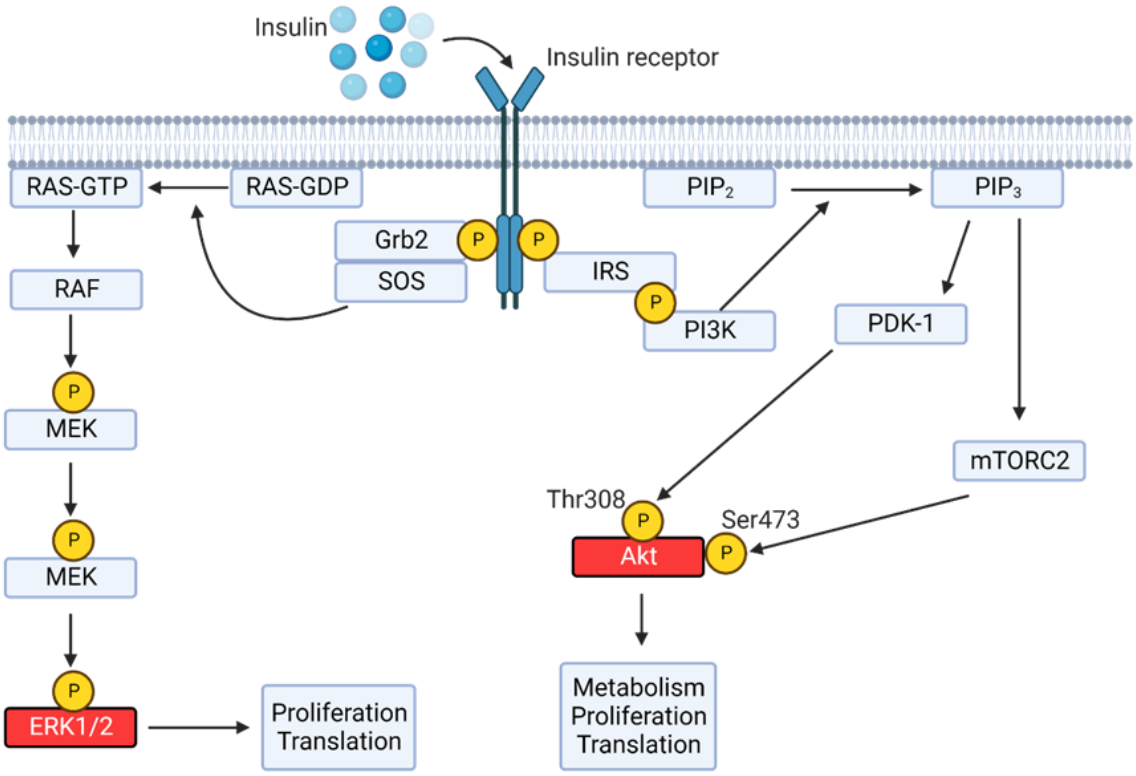

Figure 3. Insulin signaling pathways
Insulin initiates a signal transduction by binding to insulin receptor. Upon binding, insulin receptors cause autophosphorylation and conformational change to occur. This leads to recruitment of adaptor proteins such as Grb2-SOS and IRS which activates the ERK1/2 and Akt pathway, respectively. IRS recruitment to insulin receptor activates it via autophosphorylation causing the subsequent recruitment of PI3K to the membrane and the generation of PIP3. This results in recruitment and activation of PDK-1 and mTORC2 which phosphorylate Akt at Thr08 and Ser473, respectively. Immediately downstream of Grb2-SOS recruitment, RAS, RAF, and MEK are sequentially activated resulting in ERK1/2 activation.

1.5 Metabolic syndrome and diabetes

Metabolic syndrome (MetS) refers to a condition characterized by the presence of several metabolic dysfunctions which increases the risk for development of T2D, cardiovascular disease, and overall mortality [21,22]. The presence of MetS occurs when at least 3 of 5 of the following criteria (exact diagnostic thresholds shown in table 1) are met: abdominal obesity, elevated triglycerides, reduced HDL-cholesterol, increased blood pressure, and glucose intolerance. The prevalence of MetS varies by age and ethnicity, however evidence points towards an overall trend towards increased prevalence for MetS worldwide [23]. The global prevalence of metabolic syndrome is estimated to be roughly 25% [24]. MetS was once thought to be a disease that affects adults only, but the rise of MetS in younger population has also been observed [25]. Several established factors which contribute to the development of MetS include smoking, sedentary lifestyle, and overnutrition [23]. Furthermore, there is increasing evidence linking iron overload with features of metabolic syndrome [26]. In fact, there is now a condition called dysmetabolic iron overload syndrome (DIOS), which is characterized by mild elevations in body iron and is associated with MetS [27].

Table 1. Clinical definition of metabolic syndrome

The 5 criteria used in the diagnosis of metabolic syndrome are illustrated below. The definition outlined is set by the international diabetes foundation (IDF) which has been used in clinical settings worldwide [28].

Criterion	**Definition**
Abdominal obesity	Waist circumference ≥ 94 cm in men or ≥ 80 cm in women
Elevated triglycerides	150mg/dL
Reduced HDL cholesterol	<40mg/dL in men or <50mg/dL in women
Increased blood pressure	>130/85mmHg
Glucose intolerance	>100mg/dL

1.6 Mitochondrial health and insulin resistance

Mitochondria are dynamic organelles that functions to produce energy for cellular processes. Due to its central role in energy metabolism, mitochondria have gained increasing attention in metabolic diseases including T2D.

Mitochondria maintain their dynamic nature by undergoing processes of fusion and fission [8]. Collectively, the balance between mitochondrial fusion and fission is termed mitochondrial dynamics which is imperative to maintain proper mitochondrial morphology and function [8]. Upon mild stress such as at physiological conditions, mitochondria may fuse with healthy mitochondria in a process called complementation, thus re-establishing mitochondrial homeostasis [8]. However, more extreme cases such as oxidative stress can disrupt mitochondrial dynamics leading to mitochondrial dysfunction [11].

There is increasing evidence suggesting mitochondrial dysfunction plays a role in mediating a diverse range of diseases such as Alzheimer's, Parkinson disease, kidney disease, cancer, liver disease, and heart failure [29]. Moreover, due to its central role in energy metabolism, disrupted mitochondrial function and dynamics have gained increasing attention in the context of diabetes and heart disease [12]. Therefore, mitochondrial function remains an attractive therapeutic target for a diverse range of diseases, and this is reflected in the increasing number of therapeutic strategies targeting mitochondria [13].

Both mitochondrial dynamics and function are closely related. Mitochondrial dynamics has also been proposed as a bridge linking mitochondrial dysfunction and insulin resistance [30]. For instance, mitochondrial fusion is associated with improved energy metabolism whereas mitochondrial fission is associated with a decline in energy

metabolism along with elevated ROS [30]. Through mitochondrial fusion, healthy mitochondria can compensate for damaged mitochondria through sharing of mtDNA and content [31]. Due to its regulatory role in mitochondrial quality control, any major alterations in mitochondrial dynamics will be detrimental for mitochondrial health. For example, a shift from fusion to fission resulted in elevated mitochondrial ROS, impaired ß-oxidation, and impaired ATP production – all indicators of mitochondrial dysfunction [32]. Altered mitochondrial dynamics with a shift towards fission have also been observed in disease states such as insulin resistance and T2D [32,33]. When mitochondria are damaged beyond repair, such as in pathological conditions, they undergo fission followed by degradation in a process termed mitochondrial autophagy, also known as mitophagy.

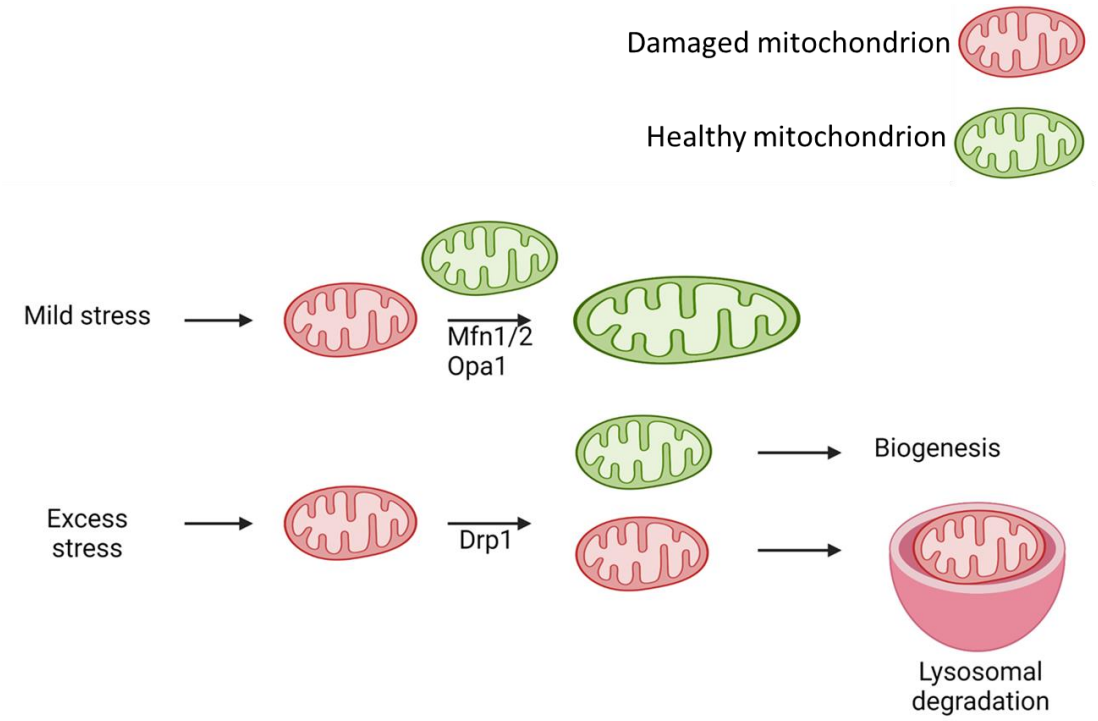

Figure 4. Mitochondrial homeostasis – fission, fusion, biogenesis, and mitophagy
Mitochondria undergo a process termed complementation where damaged mitochondria fuse with healthy mitochondria to compensate for a mild stress. This fusion process is mediated by proteins such as Mfn1, Mfn2, and Opa1. Following excess stress resulting in mitochondrial damage beyond repair, the mitochondria undergo fission, mediated by Drp1, followed by lysosomal degradation in a process called mitophagy.

1.7 Autophagy, mitophagy and insulin resistance

Mitophagy is considered a selective form of autophagy which is a catabolic process that functions to clear damaged or dysfunctional proteins and organelles [34]. The process of autophagy occurs non-specifically upon stress and can be classified into 4 distinct steps [34].

Autophagy is initiated by the formation of a double membrane structure called phagophore [35]. The phagophore is then elongated into an autophagosome, engulfing damaged organelles and proteins in the maturation process [35]. A crucial step in the maturation into an autophagosome is the lipidation of microtubule associated protein 1 light-chain 3 (LC3) into LC3-II, followed by insertion into the growing autophagosome [36]. A mature autophagosome then fuses with lysosomes, forming an autolysosomes, ultimately concluding with lysosomal degradation of damaged protein or organelles [37]. Several cargo recognition proteins are involved, the most well know being p62. P62 is an autophagy receptor that binds to cargo tagged for autophagic degradation. As such, the relative levels of p62 can be used as an indicator of the turnover rate of autophagy [36]. The protective effects of autophagy activation in insulin resistance during IO have been characterized previously [38,39]. However, the exact role of mitophagy in the induction of insulin resistance requires further investigation.

The process of mitophagy, like autophagy, relies on LC3-II and p62 in addition to several mitophagy-specific proteins. These include proteins such as PINK1/Parkin, FUNDC1, BNIP3, and Nix-mediated mitophagy.

PINK1/Parkin is the most well characterized mitophagy pathway [40]. Under physiological conditions, PINK1 is synthesized in the cytoplasm, transported to mitochondrial inner membrane, and degraded by proteases [41]. When there is mitochondrial damage or loss of membrane potential, PINK1 is stabilized on the outer mitochondrial membrane [41]. PINK1 then phosphorylates and recruits Parkin [41]. Following recruitment of Parkin, LC3 binds to parkin on LC3 interaction regions (LIRs) which mediates recruitment of vesicles called autophagosomes are recruited to mitochondria to facilitate lysosomal degradation [41].

BNIP3 and Nix mediated mitophagy are activated upon hypoxia or mitochondrial membrane depolarization [42]. Similar to Parkin, BNIP3 and Nix also contain LIRs which aid in the recruitment of autophagosomes to carry out degradation of mitochondria [42]. The FUNDC1 mitophagy receptor was identified in 2013 to contribute as a hypoxia-mediated pathway [43]. Normally, FUNDC1 is inhibited via Src phosphorylation, however, during hypoxia, Src-mediated inhibition is relieved [43]. This allows for FUNDC1 to initiate mitophagy by binding LC3 through LIR and allowing for recruitment of autophagosomes. There is a general consensus that the induction of mitophagy can improve insulin resistance [40]. However, mice with skeletal muscle-specific knockout of FUNDC1 paradoxically exhibit improved insulin sensitivity but a reduced mitochondrial energetics upon high fat diet [44]. Taken together, this suggests that the role of mitophagy in insulin resistance is highly context dependent but may be a promising target for insulin resistance.

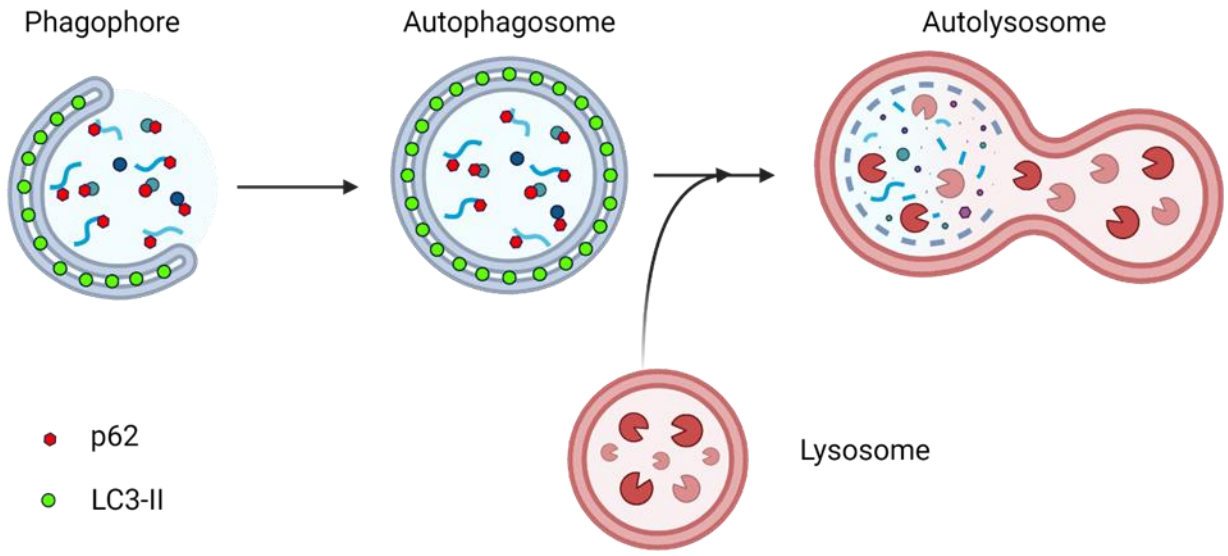

Figure 5. Process of autophagy
Autophagy is initiated by the formation of a double membrane structure called phagophore around cargo tagged by p62 which marks it for autophagic degradation. LC3-II is inserted into the growing phagophore until it matures into an autophagosome. To complete autophagy, a mature autophagosomes fuse with lysosomes to form autolysosomes where cargo along with LC3-II and p62 are proteolytically degraded.

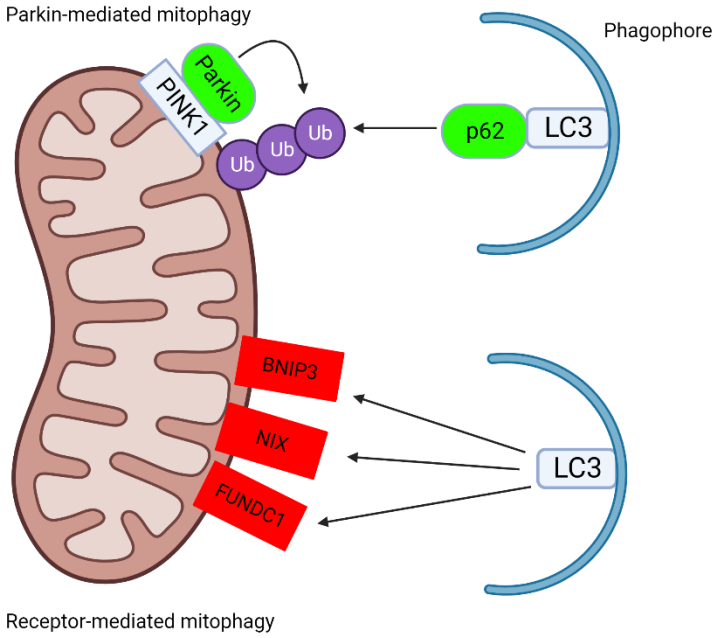

Figure 6. Process of mitophagy
Mitophagy can occur in a Parkin-dependent, or Parkin-independent (receptor-mediated) manner. Upon mitochondrial damage, PINK1 stabilizes on the outer mitochondrial membrane resulting in recruitment of Parkin and formation of ubiquitin chain. P62 binds to the growing ubiquitin chain and recruits phagophore for subsequent mitophagy. Mitophagy receptors BNIP3, NIX, and FUNDC1 contain LC3-interacting regions which directly recruits phagophore to initiate mitophagy

1.8 MitoNEET protein as a potential therapeutic target

MitoNEET (MitoN) is a transmembrane protein found on the outer mitochondrial membrane. It was originally identified as a binding target for the anti-diabetic drug, pioglitazone [45] and named after a four amino acid sequence, Asn-Glu-Glu-Thr, located near the C terminal [46]. Since its discovery in 2003, MitoN has shown potential as a novel therapeutic for a wide array diseases such as neurodegeneration, breast cancer, inflammation, cardiovascular diseases and diabetes, however, the precise mechanisms via which this occurs requires further investigations [47].

The protective effects could be attributed to mitoNEET's role in the regulation of mitochondrial iron, oxidative stress, cell death, mitochondrial health, and metabolism. For instance, MitoN knockout caused glucose intolerance, increased ROS, and dysfunctional mitochondria [46,48]. Furthermore, a decrease in MitoN expression caused a loss of mitochondrial membrane potential, leading to mitochondrial dysfunction, and subsequent apoptosis in human cancer cells [49]. In contrast, MitoN overexpression decreased mitochondrial iron and ROS [48]. MitoN has also been shown to be protective against oxidative stress-induced apoptosis by regulating mitochondrial oxidative capacity and possibly antioxidant mechanisms as well [50]. Furthermore, MitoN was found to play a role in transfer and synthesis of iron-sulfur clusters, a key factor in the function of proteins involved in cellular respiration [51]. The physiological significance of MitoN's role in iron-sulfur cluster transfer remains a topic of open discussion within the literature, however, it likely plays a role in mitochondrial function and iron homeostasis [51]. As such, MitoN likely plays a role in the development of metabolic dysfunction, however further investigation is needed to fully understand the processes involved.

1.9 Research aims and hypothesis

The link between iron overload (IO) and insulin resistance has already been established in both the cardiac setting and skeletal muscle. Furthermore, mitoNEET has also been demonstrated to have some effect in regulating mitochondrial iron. However, the link between mitochondrial iron, specifically, and insulin resistance in the cardiac setting and skeletal muscle remains largely unexplored. My objective will be to investigate the therapeutic potential of mitoNEET in IO-induced insulin resistance and the underlying mechanisms using H9c2 cardiac cells (study 1) and L6 skeletal muscle cells (study 2). Skeletal muscles are considered a classical insulin target tissue and are responsible for the majority of glucose uptake in the postprandial (fed) state. As a result, findings from the study in L6 cells could have direct implications for novel therapeutics in metabolic diseases such as T2D. In contrast, the heart is considered a non-classical insulin target tissue in that it is not the primary tissue type responsible for glucose utilization. Nevertheless, insulin resistance in the cardiac setting can have negative consequences such as the progression to cardiovascular disease including heart failure. Thus, findings from the study in H9c2 cells may have implications for therapeutics aimed at preventing cardiovascular complications in high-risk individuals.

Study 1: The role of mitoNEET in IO-induced insulin resistance in H9c2 cells

In the first study, the mechanisms underlying the protective effect of mitoNEET was investigated in IO-induced insulin resistance using H9c2 cardiac cells. Insulin resistance remains a strong risk factor for the development of T2D, which collectively increases risk for cardiovascular diseases. Early intervention of insulin resistance remains an effective

strategy to prevent the development of further difficult to treat complications. The role of mitochondrial iron in cardiac insulin resistance remains largely unexplored. I hypothesize IO in H9c2 cells will cause mitochondrial iron accumulation leading to increase in mitochondrial ROS which induces insulin resistance. I also expect regulation of mitochondrial iron through overexpression of mitoNEET in H9c2 cells will avert the deleterious effects of IO such as elevated mitochondrial ROS and insulin resistance.

Study 2: The role of mitoNEET in IO-induced insulin resistance in L6 cells

In the second study, the mechanisms underlying the protective effect of mitoNEET was investigated in IO-induced insulin resistance using L6 cells. Insulin resistance is thought to precede the onset of diabetes by up to 10 years. Because of this, early treatment of insulin resistance remains a viable option for preventing the progression to T2D. Similar to the H9c2 study, the role of mitochondrial iron, mitochondrial ROS, and protective effect of mitoNEET in insulin resistance will be explored. Furthermore, aspects of mitochondrial health including fission, fusion, biogenesis, and mitophagy will be explored as they relate to insulin resistance. Insulin resistance has been associated with an increased fission and decreased biogenesis. The precise role of mitophagy in insulin resistance is not fully clear. However, there is some evidence to suggest impaired mitophagy is linked to insulin resistance. I hypothesize during IO, L6 cells will exhibit increased mitochondrial iron accumulation, increased mitochondrial ROS, increased fission, decreased biogenesis, and decreased mitophagy. I expect these effects induced by IO will be linked to the induction of insulin resistance which can be avoided by regulation of mitochondrial iron content via overexpression of mitoNEET.

2 CHAPTER 2 – H9C2 CELLS

“MitoNEET prevents IO-induced insulin resistance in H9c2 cardiac cells through regulation of mitochondrial iron”

2.1 Abstract

Excess iron has been associated with elevated risk for type 2 diabetes (T2D) and insulin resistance. The potential role for the MitoNEET protein to regulate mitochondrial iron and preserve insulin sensitivity was examined in H9c2 cardiac cells. Extracellular iron overload (IO) was demonstrated to increase mitochondrial iron accumulation, reactive oxygen species (ROS) production, mitochondrial fission, and insulin resistance in empty vector (EV) H9c2 control cells. Under conditions of IO, overexpression of the MitoNEET (MitoN) protein was found to prevent mitochondrial iron accumulation, ROS production, mitochondrial fission, and insulin resistance. The use of mitochondrial antioxidant, Skq1, prevented IO-induced ROS production and preserved insulin sensitivity in control cells implicating mitochondrial ROS as a causal factor in the development of insulin resistance. The use of mitochondrial fission inhibitor Mdivi-1 prevented IO-induced fission but did not alter the subsequent insulin resistance in control cells. This demonstrates mitochondrial fission occurs in parallel with insulin resistance. Overall, this suggests MitoNEET plays a protective role under conditions of IO through regulation of mitochondrial iron content and ROS, thus preserving insulin sensitivity in H9c2 cells.

2.2 Introduction

Insulin resistance is one of five different metabolic defects that has been characterized in a condition called metabolic syndrome. The diagnostic criteria for metabolic syndrome is met when at least three of the following occur: hyperglycemia (high blood sugar), low levels of HDL cholesterol, elevated triglycerides, abdominal obesity, or high blood pressure. More importantly, the presence of metabolic syndrome increases the risk for developing cardiovascular diseases. Therefore, a deeper understanding of metabolic syndrome, which includes insulin resistance, in the cardiac setting may help with improving cardiovascular outcomes.

Diabetes is a common metabolic disorder affecting 8.3% of the adult population worldwide [52] and the prevalence is projected to increase 55% by 2035 [53]. Type 2 diabetes, T2D, is the most common form of diabetes, representing approximately 90% of the diabetic population. Excess iron, or IO, is an established, yet understated risk factor for the development of insulin resistance and T2D [54]. The onset of insulin resistance and T2D can have profound effects on the heart if left untreated. T2D increases the risk of developing cardiac complication such as diabetic cardiomyopathy (DCM), which is characterized by a functional decline in cardiac function, ultimately leading to heart failure and death [16]. The treatment, diagnosis, and prevention of DCM remains a challenge and as such, therapeutics targeting the treatment of insulin resistance as a preventative measure may prove to be useful [55].

Originally identified as a binding target of the antidiabetic drug pioglitazone, mitoNEET is now known to play a pivotal role in the regulation of several biological processes. MitoNEET has been implicated in regulation of mitochondrial iron and metabolism. Overexpression of mitoNEET has demonstrated to limit mitochondrial iron accumulation. MitoNEET has also been found to preserve insulin sensitivity upon high fat diet feeding in mice. Furthermore, mitoNEET has also been linked to age-related heart failure. For instance, cardiac-specific knockout of mitoNEET in mice accelerated cardiac dysfunction associated with the ageing process. Together, this suggests mitoNEET may play a protective role in preventing onset of insulin resistance under IO conditions.

In this study, an *in vitro* model of mitoNEET overexpression in H9c2 cardiomyoblasts was used to assess the role of mitochondrial iron in insulin resistance. I hypothesized that during cellular iron overload, the overexpression of mitoNEET would prevent excess mitochondrial iron accumulation resulting in preservation of insulin sensitivity. The underlying mechanisms linking mitochondrial iron and insulin resistance (mitochondrial ROS and dynamics) was also examined.

2.3 Methods

Cell culture and treatment

H9c2 cells were cultured as previously described [56]. For IO treatment, cells were treated with 200µM ferric ammonium sulfate, $NH_4Fe(SO_4)_2$, for 4 or 24 hours in serum free DMEM. Where indicated, cells were pretreated with 3µM Mdivi-1 for 3 hours, or 20nM Skq1 for 30 minutes.

MitoFerroFluor - measurement of mitochondrial iron content

MitoFerroFluor, MFF, is a fluorescent probe that is targeted to the mitochondrial matrix and exhibits a fluorescent signal that is quenched by free iron [57]. Increase mitochondrial iron loading will be observed as a decrease in MFF fluorescent signal. H9c2 EV and MitoN cells were grown on 4-well chambered coverslips overnight. Cells were treated with or without 200µM for 4 hours. Cells were washed 3 timed, then stained with 2µM MFF (a gift from Dr. John Lemasters, University of South Carolina) and nuclear mask for 30 minutes. Cells were washed 3 times, then imaged on a Nikon A1 confocal microscope. Fluorescent intensity per cell was quantified on ImageJ.

Detecting oxidative stress using CellROX™ Deep Red reagent

H9c2 EV and MitoN cells were grown on 24-well plates overnight. CellROX dye was added at a final concentration of 1µM and incubated for 30 minutes and co-stained with nuclear mask. Cells were washed 3 times then treated with or without iron overload, 200µM FAS for 4 hours. Cells were washed then imaged using EVOS™ FL Auto 2. Where indicated, cells were pretreated with mitochondrial antioxidant, 20nM Skq1, for 30 minutes. Images were capture using EVO FL Auto 2 microscope and fluorescent intensity quantified using ImageJ.

Western blot

H9c2-EV and -MitoN cells were seeded and grown to 90% confluency on 6-well plates in serum-free media, then treated with or without 200µM Ferric ammonium sulfate for 24 hours in serum free media. Where indicated, cells were treated with 100nM insulin 10 minutes prior to treatment endpoint, at which point, the cells were washed, lysed with lysis buffer (80mM Tris-HCl, 2% SDS (w/v), 15% glycerol (v/v), 10% beta-mercaptoethanol (v/v), phosphatase and protease inhibitor (A32959, Thermo Fisher Scientific, Waltham, MA, USA, and 0.1nM okadaic acid) and incubated on ice for 10 minutes. Lysates were collected, centrifuged for 15 minutes at 12000 rpm, the supernatants were collected, and heat denatured at 95°C for 5 minutes. Lysates were resolved on tris-glycine gels, transferred to PVDF membranes, blocked in 5% non-fat milk or 3% BSA, followed by incubation in primary antibodies overnight at 4°C. Membranes were washed 3 times in TBST (Tris-buffered saline with Tween 20: 20 mM Tris, 150 mM NaCl, 0.01%, w/v), incubated in appropriate secondary antibody for 1 hour, washed 3

more times in TBST, then detected with chemiluminescence on autoradiography film. Densitometric analysis was performed using ImageJ software. The following primary antibodies were used: Mfn2 (9482), Opa1 (80471), p-Drp1 S616 (3455), p-Drp1 S637 (4867), total Drp1 (8570), mitochondrial fission factor (84580), p-ERK1/2 T202/Y204 (9101), p-Akt T308 (9275), p-Akt S473 (9271), mitoNEET (83775), total Akt (9272), beta actin (12620), and GAPDH (2118) were from Cell Signaling Technology (Danvers, MA, USA). Antibodies for Mfn1 (ab221661), OXPHOS (ab110413), and mitochondrial ferritin (ab66111) were from Abcam (Cambridge, UK). Anti-PGC1α (NBP1-04676) was from Novus Biologicals (Englewood, CO, USA). Anti-Fis1 (sc-376447) was from Santa Cruz. Anti-mouse and anti-rabbit HRP-linked secondary antibodies were from Cell Signaling Technology.

Mitochondrial network analysis

H9c2 EV and MitoN cells were seeded on 4-well chambered coverslips overnight. Cells were treated with or without 200μM FAS for 24 hours. Mitotracker green, 50nM (Thermo Scientific), and nuclear mask staining was added 30 minutes before treatment endpoint. Cells were washed, changed to phenol free DMEM, and imaged on A1 confocal microscope. Images were captured at 60x magnification and zoomed in 3x. Network branch length (mitochondrial length), network branches (degree of mitochondrial networking), and mitochondrial footprint (mitochondrial area) per cell were quantified using ImageJ mitochondrial network analysis tool [58]. For 3D images, Z-stacks were captured using 0.2μm step size, then rendered using the surfaces algorithm on IMARIS software (Oxford Instruments, Abingdon, US).

MitoNEET overexpressing cell line

Generation and selection of a stable MitoN overexpressing cell line was described previously [56].

Statistical Analysis

Data is shown as mean ± SEM. One way ANOVA followed by Tukey's multiple comparison test or t-test was used for statistical analysis. All statistical tests were performed using GraphPad Prism. $p<0.05$ was considered statistically significant.

2.4 Results

IO-induced insulin resistance is prevented by mitoNEET

The MitoN overexpressing cell model was established in a previous publication where there was about 2.5-fold increase in MitoN protein. [56]. MitoN overexpression was utilized to selectively regulate mitochondrial iron during conditions of IO. Mitochondrial ferritin is an iron storage protein that is translationally repressed by IRPs under physiological conditions, however excess mitochondrial iron will relieve this repression. Because of this, an elevated level of mitochondrial ferritin can be used as an indicator of increased mitochondrial iron content. By western blot, it was determined that IO caused a significant increase in mitochondrial ferritin in EV control, but not in MitoN cells (Fig. 1A). This was also confirmed in live cell imaging using MitoFerroFluor (MFF), a fluorescent probe targeted to the mitochondria which has its fluorescence quenched by iron. Following IO, MFF fluorescent signal decreased nearly 50% in EV, but remained largely unchanged in MitoN cells (Fig. 1B,C).

One of the key downstream effector proteins during insulin signaling is Akt, which is activated following insulin stimulation via phosphorylation at T308 and S473. The phosphorylation status of Akt was quantified as a measurement of insulin signaling. In H9c2 EV control cells, IO significantly blunted insulin-stimulated phosphorylation of Akt at T308 and S473, indicative of insulin resistance. In the H9c2 MitoN cells, insulin stimulated phosphorylation of Akt remained largely unchanged suggesting preserved insulin sensitivity. Extracellular regulated kinase 1/2 (ERK1/2) is another protein activated by phosphorylation upon insulin signaling. ERK1/2 activation originates also from IRS, but it diverges from the Akt pathway. Thus, phosphorylated ERK1/2 can serve as an

additional indicator of insulin sensitivity. In H9c2 EV cells, IO decreased insulin-stimulated phosphorylation of ERK1/2 suggestive of insulin resistance (Fig 1F). This reduced phosphorylation was not seen in the H9c2 MitoN IO-treated cells (Fig 1F). Together, this data demonstrated that IO caused significant insulin resistance which was prevented by MitoN overexpression.

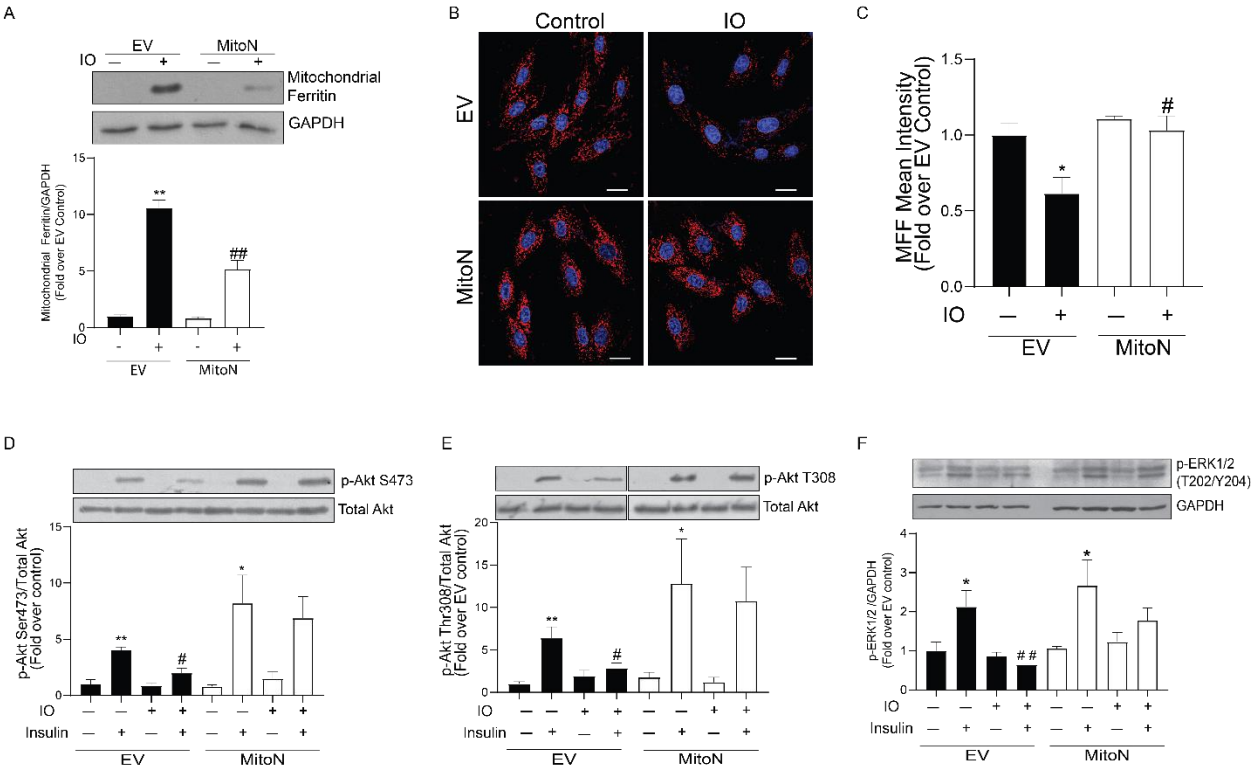

Figure 1. IO-induced insulin resistance is prevented by mitoNEET. **(A)** Evaluation of mitochondrial iron overload by Western blot analysis of mitochondrial ferritin in H9c2-EV and -MitoN cells treated with (IO) or without (control) iron for 24 hours. Representative blot and loading control are shown, n=4. **p<0.01 compared to EV control, ##p<0.01 compared to EV IO **(B, C)** Quantification of relative mitochondrial iron content using MFF in H9c2-EV and -MitoN cells treated with (IO) or without (control) iron for 4 hours. Representative confocal images are shown in B and quantified in C using ImageJ software. n=3. Scale bar = 20μm. *p<0.05 compared to EV control, #p<0.05 compared to EV IO. Insulin signaling assessed by Western blot analysis of **(D)** p-Akt S473, **(E)** p-Akt T308, and **(F)** p-ERK1/2 in H9c2-EV and -MitoN cells treated with (IO) or without (control) iron for 24 hours. Representative blots of p-Akt S473 (n=5) and p-Akt T308 (n=10) with loading controls are shown. *p<0.05 compared to EV control, **p<0.01 compared to EV control, #p<0.05 compared to EV IO.

IO-induced oxidative stress is prevented by mitoNEET

Having established the protective role of MitoN in IO-induced insulin resistance, oxidative stress was subsequently examined. CellROX red is a fluorescent probe that is weakly fluorescent in the reduced state but is highly fluorescent following oxidation by ROS. It was found that IO induced significant ROS production in H9c2 EV control cells (Fig. 2A-B). Pre-treatment with mitochondrial antioxidant Skq1 attenuated this IO-induced ROS production suggesting IO-induced ROS is derived primarily from mitochondria. Furthermore, in H9c2 MitoN cells, IO treatment induced a significantly lower level of ROS compared to EV cells. To determine if IO-induced ROS played a causative role in the development of insulin resistance, western blot analysis for Akt phosphorylation in the presence of Skq1 was performed in H9c2 EV control cells. The data showed IO caused significant insulin resistance that was completely prevented by Skq1 (Fig 2C,D). Collectively, IO caused mitochondrial ROS upregulation leading to insulin resistance, but this was prevented by mitochondrial antioxidant, Skq1, or MitoN overexpression.

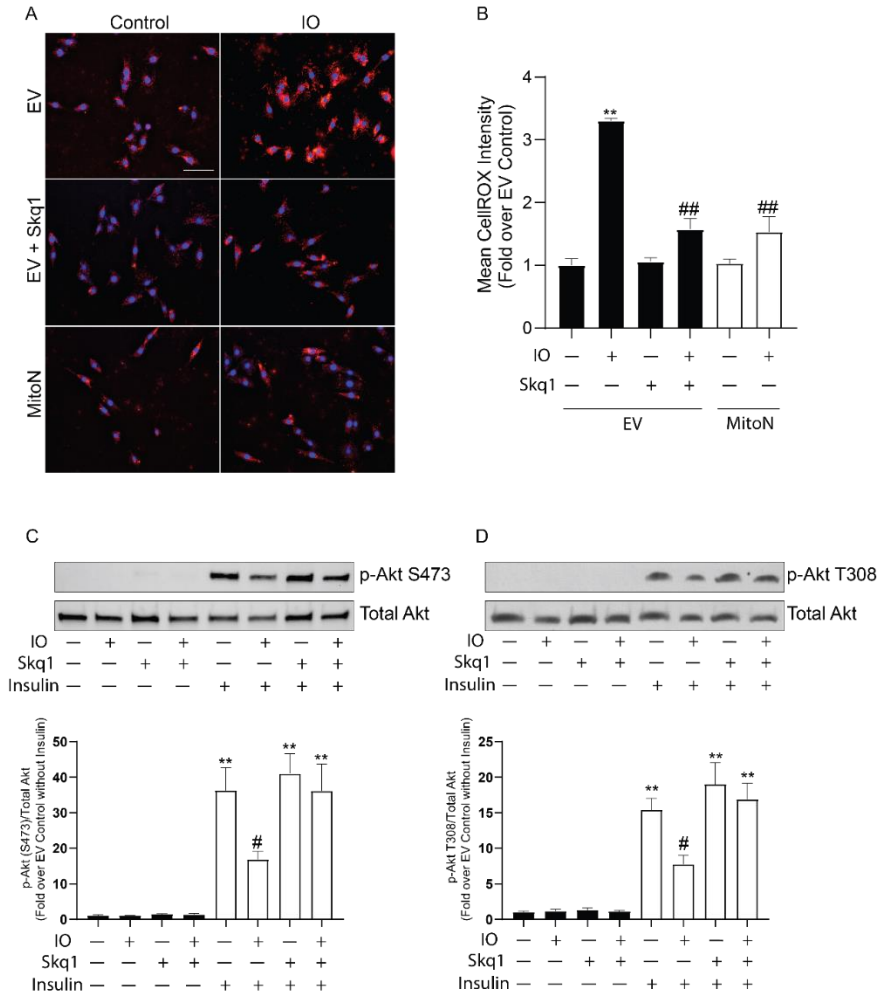

Figure 2. IO-induced oxidative stress is prevented by mitoNEET. **(A, B)** Reactive oxygen species (ROS) production was quantified using CellROX in H9c2-EV and -MitoN cells treated with (IO) or without (control) iron for 4 hours. Representative fluorescent images are shown in A and quantification by ImageJ software in B, n=3. Scale bar = 100µm. **p<0.01 compared to EV control, ##p<0.01 compared to EV IO. **(C, D)** Assessment of insulin signaling by Western blot analysis of p-Akt S473 (n=5) and p-Akt T308 (n=6) in H9c2-EV cells treated with (IO) or without (control) iron for 24 hours. Where indicated, cells were pretreated with mitochondrial antioxidant, Skq1 for the entire 24 hours. **p<0.01 compared to EV control, #p<0.05 compared to EV IO.

IO-induced mitochondrial fragmentation is prevented by mitoNEET

Oxidative stress has been linked with fragmented mitochondria, and whether this played a role in IO-induced insulin resistance was investigated. Fragmented mitochondria can arise from decreased fusion, increased fission, or a combination of both. To assess for fusion, western blot analysis of fusion-related proteins (Opa1, Mfn1, and Mfn2) was performed where there was no change found following IO (Fig A-C). Dynamin related protein 1 (Drp1) is a key protein involved in fission where upon phosphorylation at S616, fission is promoted, whereas phosphorylation at S637 inhibits it. In H9c2 EV cells, IO was found to increase the phosphorylation ratio of S616:S637 indicative of elevated fission (Fig 3D). However, this increased was not observed in H9c2 MitoN cells (Fig 3D). Drp1-mediated fission can occur through different pathways depending on which Drp1 receptor is involved. Two known Drp1 receptors, mitochondrial fission factor (mtff) and fission protein 1 (Fis1) were characterized. Although both mitochondrial fission factor and Fis1 promote fission via Drp1, they were found to be functionally distinct. Mitochondrial fission factor mediated fission precedes biogenesis and proliferation, whereas Fis1 mediated fission is followed by degradation. This duality may indicate mtff-dependent fission is involved in the maintenance of mitochondrial networks. In contrast, Fis1-dependent fission may act as a marker for mitochondria damaged beyond repair and may be implicated with disease progression. Mitochondrial fission factor was largely unchanged across all conditions (Fig 3E). In H9c2 EV, IO increased Fis1, but this was not observed in H9c2 MitoN cells (Fig 3F).

Elevated levels of fission were then visually corroborated by staining cells with Mitotracker green, a fluorescent dye that specifically stains mitochondria independent of membrane potential. Mitochondrial length and branching were quantified and found to be reduced by IO (indicating elevated fission) in H9c2 EV cells, but not in H9c2 MitoN cells (Fig 3G). Mitochondria were also analyzed using Mitotracker and IMARIS software to quantify sphericity (the ratio of the surface area of a sphere to the surface area of an object, of the same volume, will approach 1 as the object approaches the shape of a sphere). In H9c2 EV, IO significantly increased sphericity of mitochondria indicative of elevated fission. In H9c2 MitoN cells, mitochondrial sphericity remained unchanged following IO compared to control (Fig 3I).

Next, it was determined whether fission played a causal role in IO-induced insulin resistance. IO-induced fission was modulated through the use of Mdivi-1, a pharmacological inhibitor of Drp1 activity. In H9c2 EV, IO decreased mitochondrial length and branching which was averted when the cells were pretreated with Mdivi-1 (Fig 3J). The effect of Mdivi-1 on IO-induced insulin resistance was investigated by western blot analysis of Akt phosphorylation. In H9c2 EV cells, IO was found to cause insulin resistance and the use of Mdivi-1 did not prevent this (Fig 3K). This shows IO induces mitochondrial fission via the Fis1-Drp1 pathway, however, the inhibition of Drp1 activity did not prevent the following insulin resistance.

Additional aspects of mitochondrial health such as mitochondrial content, mitochondrial DNA copy number, and mitophagy were investigated but the findings were inconclusive. The data has been included in the final publication for completeness but was not included here.

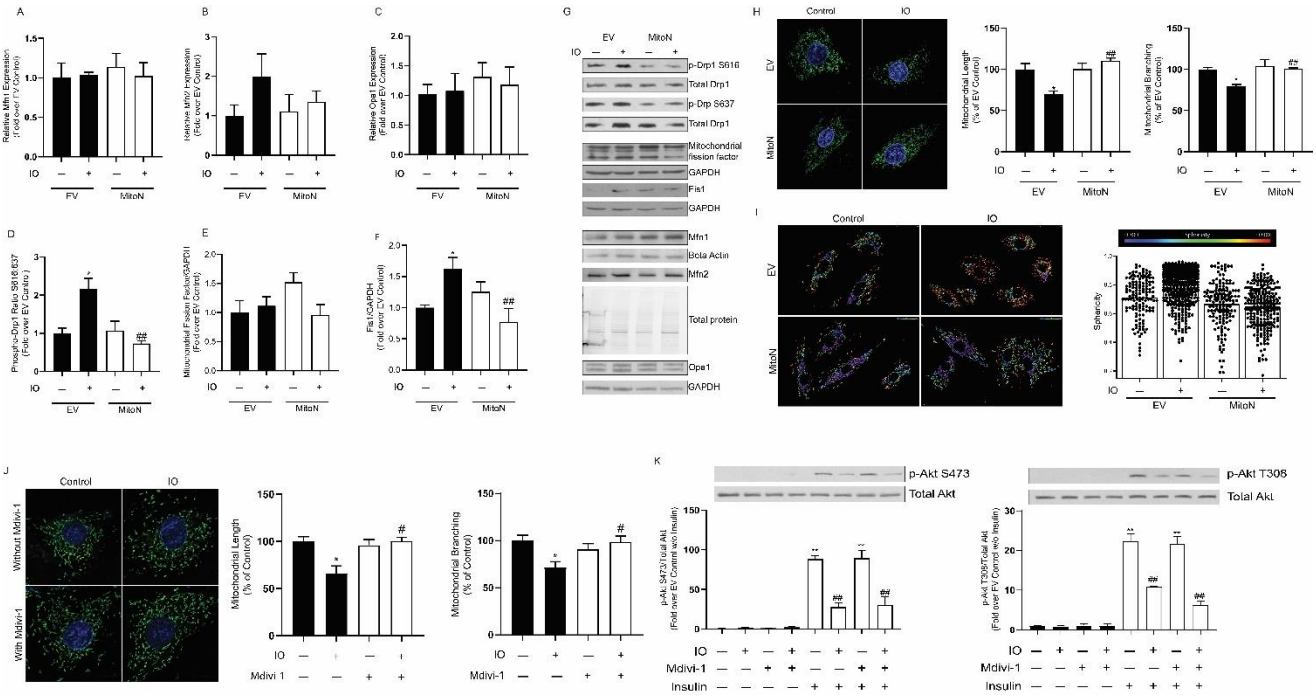

Figure 3. IO-induced mitochondrial fragmentation is prevented by mitoNEET. **(A - C)** Quantification of mitochondrial fusion proteins, Mfn1 (n=5), Mfn2 (n=4), and Opa1 (n=3), assessed by Western blot analysis in H9c2-EV and -MitoN cells treated with (IO) or without (control) iron for 24 hours. **(D - F)** Assessment of mitochondrial fission related proteins by Western blot analysis of the Drp1 phosphorylation ratio pS616:pS637 (n=3), mitochondrial fission factor (n=3), and Fis1 (n=6) in H9c2-EV and -MitoN cells treated with (IO) or without (control) iron for 24 hours. **(G)** Representative blots of fusion and fission proteins with loading control are shown. **(H)** Quantitative analysis of mitochondrial networks using Mitotracker green in H9c2-EV and -MitoN cells treated with (IO) or without (control) iron for 24 hours. Representative fluorescent images of mitochondria are shown and quantification of mitochondrial length and branching by ImageJ software are adjacent, n=3. Scale bar = 10µm. **(I)** 3D images of mitochondrial networks processed with the Imaris software sphericity quantification tool (using the surfaces algorithm) is shown in H9c2-EV and -MitoN cells treated with (IO) or without (control) iron for 24 hours. Quantification is representative of at least 134 mitochondria. Scale bar = 5µm. **(J)** Quantitative analysis of mitochondrial length and branching using ImageJ software analysis of Mitotracker green fluorescence in H9c2-EV cells treated with (IO) or without (control) iron for 24 hours. Where indicated, cells were pretreated with Drp1 inhibitor, Mdivi-1. Representative images are shown, n=3. Scale bar = 10µm. **(K)** Assessment of insulin signaling by Western blot analysis of p-Akt S473 and p-Akt T308 in H9c2-EV cells treated with (IO) or without (control) iron for 24 hours. Where indicated, cells were pretreated with Drp1 inhibitor, Mdivi-1. Representative blots with loading controls are shown, n=3. *p<0.05, **p<0.01 compared to EV control; #p<0.05, ##p<0.01 compared to EV IO.

2.5 Discussion

Insulin resistance is a known risk factor for complications including T2D and cardiovascular diseases. In fact, signs of insulin resistance have been observed in humans up to 10 years prior to the development of T2D [59]. As a result, therapies aimed at treating insulin resistance are appropriate for early intervention against T2D and cardiovascular diseases. The role IO plays in causing insulin resistance has been previously described in the literature [39]. However, the effects of mitochondrial iron, specifically, has not been fully defined.

In this study, an H9c2 cell line overexpressing the MitoN protein was used to investigate its therapeutic potential in mitigating insulin resistance under conditions of iron overload. In IO-treated H9c2 cells, MitoN overexpression prevented accumulation of mitochondrial iron as compared to H9c2 EV cells as shown by MFF staining. Furthermore, mitochondrial iron was significantly upregulated by IO in EV, but not MitoN cells. Following IO, EV cells displayed signs of insulin resistance, however, MitoN cells exhibit normal insulin signaling action, demonstrating it played a protective effect against insulin resistance.

Oxidative stress has been known to play a role in the pathogenesis of T2D and its associated cardiovascular complication [60]. Nevertheless, studies investigating the therapeutic potential of general antioxidants generally concluded them to be ineffective at treating T2D and cardiovascular complications [61,62]. Using CellROX, the role of oxidative stress in IO-induced insulin resistance in H9c2 cells was explored. IO caused an increase in ROS, which could be avoided with MitoN overexpression, or with the mitochondrial antioxidant Skq1. This indicates mitochondria are a major contributor of

cellular ROS during conditions of IO. Moreover, Skq1 was demonstrated to provide complete protection against IO-induced insulin resistance as measured by insulin-stimulated Akt phosphorylation. Thus, targeting mitochondrial ROS specifically, may be a more useful therapeutic strategy in protecting against cardiac insulin resistance.

Elevated levels of mitochondrial fission have been associated with the development of insulin resistance [32]. Furthermore, mitochondria from patients with T2D or heart failure were found to be smaller, suggesting increased mitochondrial fission [63,64]. In H9c2 EV, but not MitoN cells, IO was found to increase S616:S637 phosphorylation ratio of Drp1, indicative of increased fission. Furthermore, the IO-induced fission was found to proceed through the Fis1-pathway, but not the mitochondrial fission factor pathway. The Fis1 -dependent fission is characterized by mitochondria marked for degradation and may be linked with a pathological state. Visual analysis of mitochondria by Mitotracker green staining corroborated the increased Drp1 activity where mitochondria from IO-treated H9c2 EV, but not MitoN, were more fragmented. The data presented, however, demonstrated IO-induced mitochondrial fission did not contribute to insulin resistance. The use of the selective Drp1 inhibitor, Mdivi-1, prevented fission, but did not preserve insulin sensitivity following IO.

In conclusion, this study characterized the role of mitochondrial iron in the pathogenesis of insulin resistance in H9c2 cardiac cells. During IO, mitochondrial iron was elevated which led to an induction of mitochondrial ROS, and consequently insulin resistance. Moreover, it was shown that the MitoNEET protein was protective against IO-induced insulin resistance. The protective effect of MitoNEET is mediated via its ability to regulate mitochondrial iron, therefore preventing IO-induced mitochondrial ROS and the subsequent insulin resistance in H9c2 cells (summarized in Figure 4).

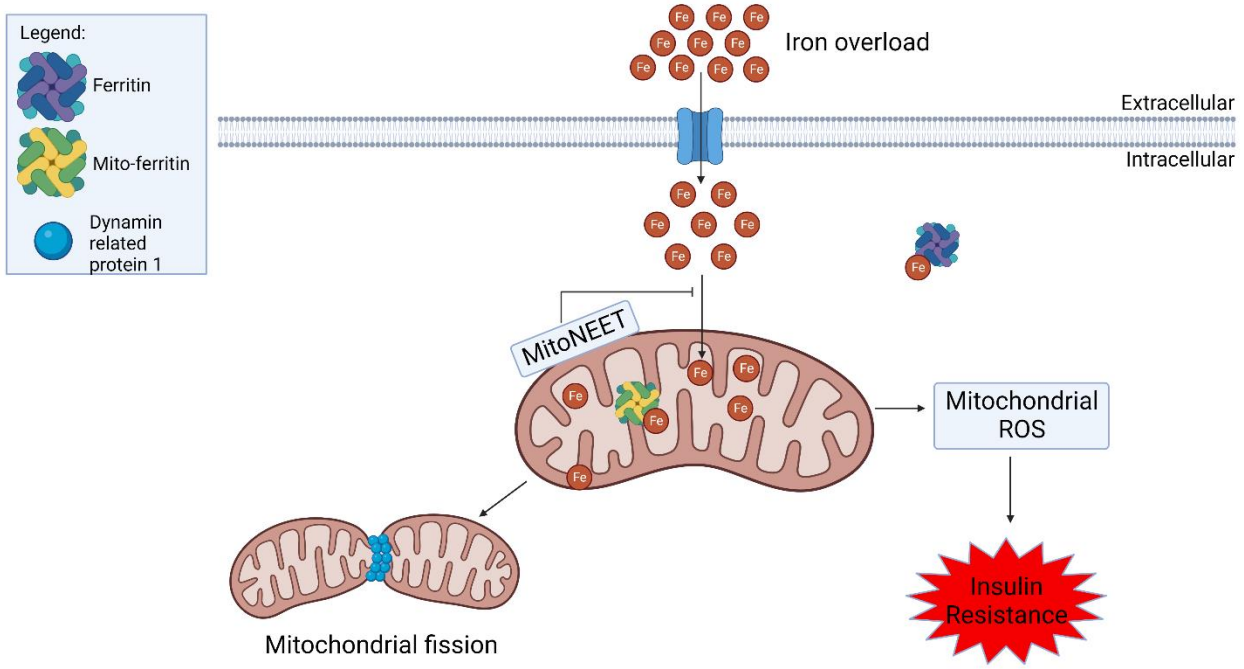

Figure 4. Protective role of MitoNEET during iron overload. Extracellular iron overload (IO) led to increased mitochondrial iron accumulation. A modest surplus of iron can be stored in iron storage proteins called ferritin in the cytosol or mitochondria. IO induced an increase in mitochondrial ROS which was causally linked to the development of insulin resistance. IO also induced an increase in mitochondrial fission, but this was not causally linked to the onset of insulin resistance.

3 CHAPTER 3 – L6 CELLS

“MitoNEET prevents IO-induced insulin resistance in L6 skeletal muscle cells through regulation of mitochondrial iron”

3.1 Abstract

Iron overload (IO) is known to contribute to metabolic dysfunction such as type 2 diabetes and insulin resistance. Using L6 skeletal myoblasts, we examined the role of MitoNEET as a potential therapeutic against IO-induced insulin resistance. First, the *in vitro* model of IO-induced insulin resistance was established using an Akt biosensor cell line and by western blot analysis of Akt phosphorylation. IO resulted in accumulation of iron within the mitochondria as shown by fluorescent probe, MitoFerroFluor (MFF), and elevated levels of iron storage protein, mitochondrial ferritin. Accumulation of mitochondrial iron subsequently caused an upregulation of mitochondrial ROS as shown by MitoSOX staining. IO was also found to increase mitochondrial fission via the fission protein 1 (Fis1) pathway shown by western blot and analysis of mitochondrial networks. Mitochondria-specific antioxidant, Skq1, prevented IO from upregulating fission indicating this process is dependent on mitochondrial ROS. A cell line overexpressing the mitochondrial membrane protein, MitoNEET, was generated to regulate levels of mitochondrial iron. Therefore, MitoNEET overexpression could prevent insulin resistance through regulation of mitochondrial iron, mitochondrial ROS, and fission under conditions of excess iron.

3.2 Introduction

Iron plays a crucial role in different metabolic processes such as oxygen transport, cellular respiration, and electron transport [65]. However, an excess of iron, termed iron overload (IO), has been shown to lead to conditions such as insulin resistance and type 2 diabetes (T2D) [38,66]. An excess of iron leads to the production of reactive oxygen species (ROS), causing oxidative stress which is known to directly cause insulin resistance [60]. Treatments aimed at regulating excess iron has shown some benefit in improving insulin resistance and T2D, however, limitations exist. For instance, iron chelation has shown to be beneficial in improving insulin sensitivity in an animal model of obesity [67]. However, long term iron chelation therapy in humans has been known to cause visual and auditory toxicity [68]. Furthermore, iron chelation therapy alone may not be sufficient to entirely mitigate the detrimental effects of iron overload [69].

The redox-active iron that accumulates following IO, termed labile iron pool (LIP), was once thought to be primarily cytosolic [70]. However, studies have shown this cytosolic LIP can be redistributed to organelles such as lysosomes and mitochondria [71,72]. An excess of iron accumulation within mitochondria has gained increasing attention for its potential role in mediating insulin resistance [73]. Mitochondrial iron import across the inner membrane is mediated by mitoferrin proteins, however, import across the outer membrane is not well characterized [74]. Nevertheless, the regulation of mitochondrial iron is a more targeted approach and may produce more effective outcomes.

Mitochondria are dynamic organelles that play an indispensable role in energy metabolism [75]. Mitochondrial dynamics, referring to the two opposing processes of fusion and fission, help maintain mitochondrial homeostasis. Fusion is mediated by mitofusins 1 and 2 (mfn1/2) , optic atrophy a (Opa1). Fission is mediated by the GTPase, dynamic related protein 1 (Drp1), where it is recruited to mitochondria by different receptors including mitochondrial fission factor, fission protein 1 (Fis1), mitochondrial dynamics proteins of 49 and 51 (MiD49 and MiD51) [76]. Due to its central role in energy metabolism, it comes as no surprise that dysfunctional mitochondria have been implicated in metabolic disorders such as insulin resistance and T2D [77]. Several aspects of mitochondrial dysfunction have been explored in how it contributes to insulin resistance. For one, mitochondria are a major source of ROS and if left unregulated, can lead to oxidative stress [78]. Dysregulated production of ROS can arise from an external stress stimuli, or from dysfunctional mitochondria [79]. That subsequently causes an increase in electrons leaking out of the electron transport chain, which react with oxygen to form ROS [79]. An increase in ROS further exacerbates mitochondrial dysfunction, further increasing ROS in a cycle, ultimately causing insulin resistance [80].

Aberrant mitochondrial dynamics may provide a possible link between mitochondrial dysfunction and insulin resistance [81]. Overexpression of fusion-related proteins mitofusin 1 (Mfn1) or mitofusin 2 (Mfn2) were found to be beneficial in improving insulin sensitivity in a diabetes-susceptible cell model [81]. On the other hand, overexpression of Fis1 and Drp1 had an adverse effect on insulin signaling [81]. Furthermore, mitochondria in skeletal muscle from humans with insulin resistance or T2D

exhibit lower density, number, and a reduced expression of Mfn2 [82–84]. Collectively, this implicates abnormal mitochondrial dynamics in the development of insulin resistance.

MitoNEET is an iron-sulfur (Fe-S) transmembrane protein found in the outer mitochondrial membrane [48]. MitoNEET is a regulator of mitochondrial iron homeostasis, possibly via transfer of Fe-S clusters from the mitochondria to acceptors such as iron regulatory protein 1 (IRP1) [85]. MitoNEET overexpression has been shown to be beneficial in preserving insulin sensitivity in models of obesity [46]. This was associated with reduced mitochondrial iron content, lower ROS, decreased ETC activity, and fatty acid oxidation [11]. MitoNEET was also found to maintain mitochondrial networks, further suggesting it plays a role in mitochondrial function [86].

Using an *in vitro* model of IO, we examined the role of mitochondrial iron accumulation in insulin resistance in L6 skeletal muscle cells. We show that mitochondrial iron accumulation led to an upregulation of mitochondrial fission and ROS, and subsequently insulin resistance. To regulate mitochondrial iron, a cell line overexpressing MitoNEET was created. Regulation of mitochondrial iron content by MitoNEET overexpression inhibited the upregulation of mitochondrial fission, ROS, and insulin resistance caused by IO.

3.3 Materials and methods

Cell culture and treatment

Cell culture methods are described previously [38]. For iron overload (IO), L6 cells were treated with 250μM ferrous ammonium sulfate (FAS) diluted in AMEM containing 0.5% FBS and 1% antibiotic/antimycotic for 4 hr or 24 hr. Mitochondrial antioxidant, Skq1 (20nM), or fission inhibitor, Mdivi-1 (3μM) was added 30 minutes prior to treatment.

Generation of L6 MitoNEET overexpressing and Akt biosensor and cells

MitoNEET overexpressing, empty vector (EV) control, and Akt biosensor cells were generated as previously described [56,87].

Western blot

L6 cells were seeded and grown to 90% confluency in 6-well plates. Following treatment (250μM FAS, 24 hr), cells were lysed on ice using lysis buffer containing protease and phosphatase inhibitors. Where indicated, 100nM insulin was added 10 minutes prior to treatment endpoint. Samples were denatured at 95°C for 5 minutes, resolved using SDS-PAGE, and transferred to PVDF membrane. Membranes were blocked with 3% BSA or 5% milk for 1 hr. Membranes were incubated at 4°C overnight in primary antibodies. Membranes were washed 3 times in TBST, then incubated in the appropriate secondary antibody. Enhanced chemiluminescent signal was detected using X ray film and quantified using ImageJ. Antibodies information are as follows. Fis1 (1:100) was from Santa Cruz Biotechnology. PGC1α (1:1000) was from Novus Biologicals. P62 (1:1000) was from Biorad. Mitochondrial ferritin (1:1000), mfn1 (1:1000), and Parkin

(1:1000) was from Abcam. mitoNEET (1:1000), p-Akt S473 (1:1000), p-Akt T308 (1:1000), total Akt (1:1000), p-Drp1 S616 (1:500), p-Drp1 S637 (1:500), total Drp1 (1:1000), mitochondrial fission factor (1:1000), mfn2 (1:500), Opa1 (1:1000), LC3 (1:1000), and GAPDH (1:1000) were from Cell Signaling Technology.

Mitochondrial iron quantification

MitoFerroFluor, MFF (a kind gift from Dr John J. Lemasters), was used to monitor mitochondrial iron content. MFF selectively accumulates in mitochondria where it presents a fluorescent signal that is quenched by iron. L6 cells were seeded at 70% confluency in 4-well chambered polymer coverslips and allowed to grow overnight. Following treatment (250µM FAS, 4 hr), cells were washed 3 times, then incubated with 2µM MFF and nuclear stain for 30 minutes in serum free AMEM at 37°C protected from light. Following 3 more washes, cells were imaged using a Nikon A1 confocal microscope with an incubator (37 °C, 5% CO_2). Mean MFF intensity was quantified using ImageJ.

Mitochondrial reactive oxygen species quantification

MitoSOX is a fluorescent probe that is targeted to mitochondria and increases in signal upon oxidation by ROS. L6 cells were seeded at 70% confluency in 4-well chambered polymer coverslips and allowed to grow overnight. Following treatment (250µM FAS, 4 hr), cells were incubated with 5µM MitoSOX red and nuclear stain for 30 minutes in serum free AMEM at 37°C. Following 3 washes, cells were imaged using a Nikon A1 confocal microscope with an incubator (37 °C, 5% CO2). Mean MitoSOX intensity was quantified using ImageJ.

Mitochondrial network visualization and analysis

L6 cells were seeded at 60% confluency in 4-well chambered polymer coverslips and allowed to grow overnight. Following treatment (250µM FAS, 24 hr), cells were washed 3 times, then incubated with 100nM Mitotracker green and nuclear stain for 30 minutes in serum free AMEM at 37°C protected from light. Following 3 more washes, cells were imaged using a Nikon A1 confocal microscope with an incubator (37 °C, 5% CO2). Mitochondrial branch length and networking were quantified as described in the literature to assess fission in 2D [58]. For 3D images, z-stacks were captured with a step size of 0.2µm and rendered using surfaces tool on IMARIS.

Statistics

Data are presented as mean ± SEM. One-way analysis of variance followed by Tukey's multiple comparison test or student's t-test was used in GraphPad Prism. Statistical significance was determined to be $p<0.05$.

3.4 Results

MitoNEET prevents mitochondrial iron accumulation and insulin resistance following IO

An L6 cell line stably overexpressing the MitoNEET (MitoN) protein was generated to selectively modulate mitochondrial iron content in an *in vitro* model of IO. Stable overexpression of MitoN was validated by western blot where the MitoN cell line expressed a significantly higher level of MitoN protein compared to the empty vector (EV) control cell line (Fig 1A). The transfected MitoN proteins (arrow) migrated slower than the endogenous MitoN due to presence of a FLAG tag (~1kDa). To measure the amount of mitochondrial iron accumulation upon IO, the relative protein levels of mitochondrial ferritin was quantified by western blot. Mitochondrial ferritin is an iron storage protein that is translationally upregulated by iron and can therefore be used as an indicator of mitochondrial iron accumulation. IO was found to significantly increase mitochondrial iron accumulation, which was prevented by MitoN overexpression (Fig 1B). These findings were further corroborated using MitoFerroFluor (MFF) staining, a fluorescent sensor of iron. MFF accumulates in mitochondria and is retained independent of membrane potential by forming covalent bonds with mitochondrial proteins [57]. MFF fluorescence is quenched by iron, but not other biological cations such as calcium [57]. As such, mitochondrial iron accumulation can be examined by quantification of MFF fluorescence intensity. IO was found to quench MFF fluorescence by more than 50% in EV cells, while MFF fluorescence remained unchanged in MitoN cells, indicating MitoN overexpression can prevent mitochondrial iron accumulation (Fig 1C, D). Insulin signaling was assessed by insulin stimulated phosphorylation of Akt at S473 and T308. IO was found to

significantly blunt insulin stimulated phosphorylation of Akt at both S473 and T308 in EV cells, indicative of insulin resistance (Fig 1E). MitoN overexpression prevented the deleterious effects of IO on insulin signaling (Fig 1E). These findings were further corroborated by measuring Akt activity using an Akt biosensor cell line containing a GFP-tagged FOXO1 (Fig 1F). Complete activation of Akt activity is mediated by phosphorylation at both S473 and T308 which then phosphorylates the FOXO1 transcription factor causing its nuclear export into the cytosol. Nuclear GFP intensity can be quantified in real-time as an indicator of Akt activity following insulin stimulation. When insulin signaling is preserved, insulin stimulation causes a rapid decrease in nuclear GFP intensity as seen in both EV and MitoN insulin control (Fig 1F, G). IO was found to inhibit Akt activity in EV cells which is shown as a sustained higher intensity of nuclear GFP following insulin stimulation over time (Fig 1F). MitoN overexpression preserved Akt activity following IO (Fig 1F, G), similar to the conclusions found by western blot analysis of p-Akt.

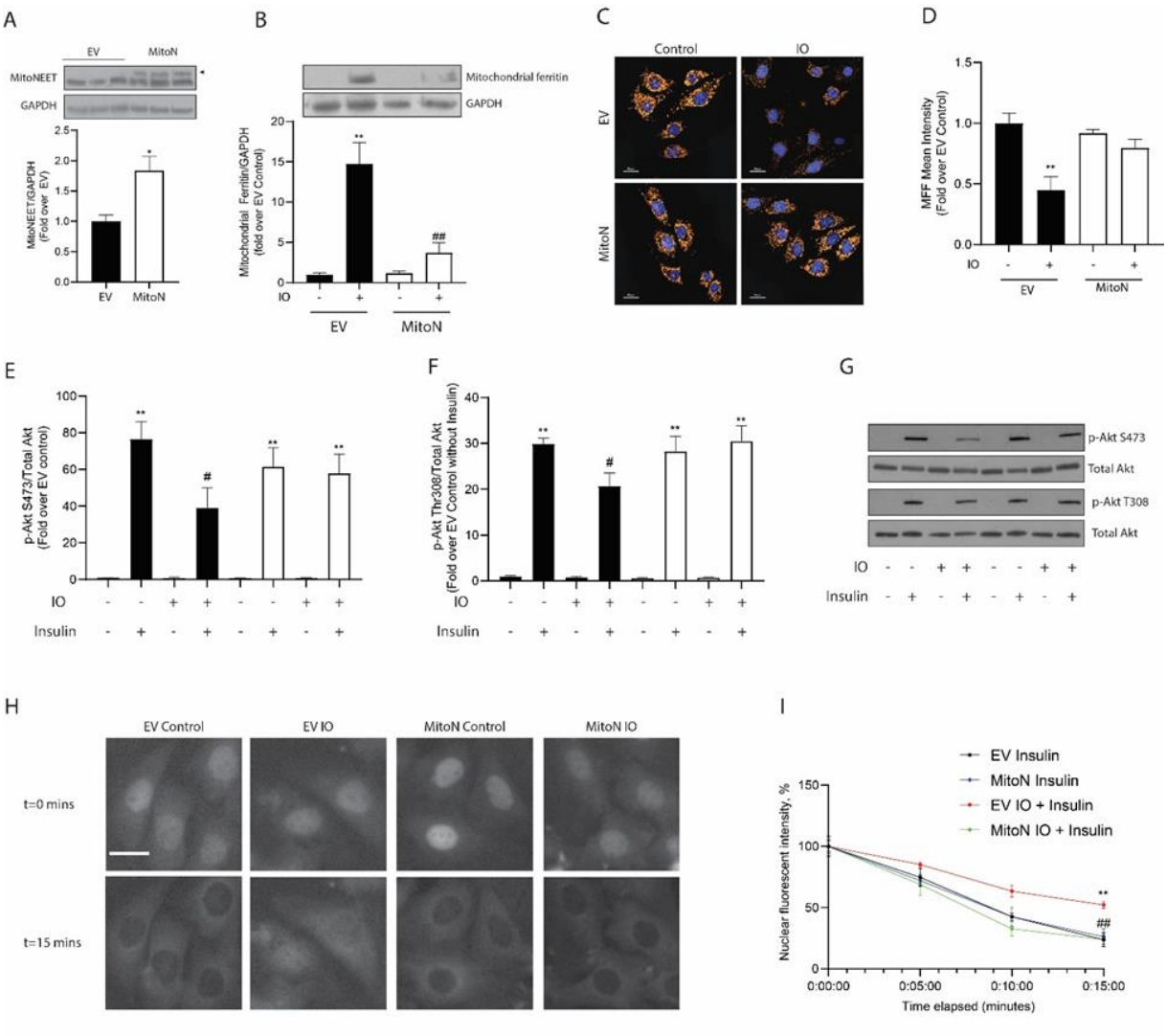

Figure 1. MitoNEET prevents mitochondrial iron accumulation and insulin resistance following IO. **(A)** Validation of MitoNEET overexpression (transfected MitoNEET indicated by arrow) in L6 cells by western blot analysis. Representative blot with loading control is shown, n=6. **(B)** Western blot analysis of mitochondrial ferritin, indictor of mitochondrial iron content, in L6 EV and MitoN cells treated with (IO) or without (control) iron for 24 hours. Representative blot and loading control are shown, n=5. **(C, D)** Measurement of mitochondrial iron by MFF staining in L6 EV and MitoN cells treated with (IO) or without (control) iron for 4 hours. MFF fluorescent images representative of n=3 is shown, scale bar = 20µm. Western blot of **(E)** p-Akt S473 (n=5) and **(F)** T308 (n=7) in L6 EV and MitoN cells treated with (IO) or without (control) iron for 24 hours. Representative blots with loading control are shown. **(H)** L6 EV or MitoN Akt biosensor cells treated with (IO) or without (control) iron for 24 hours. **(I)** Representative fluorescent images are shown, n=3. Scale bar = 20µm. *Indicates significant difference compared to EV control, $p<0.05$. **Indicates significant difference compared to EV control, $p<0.01$. #Indicaites significant difference compared to EV IO, $p<0.05$. ##Indicates significant difference compared to EV IO, $p<0.01$.

MitoNEET prevents IO-induced mitochondrial fragmentation

Because mitochondrial fission has been associated with insulin resistance, mitochondrial fission was examined in this cellular model of IO. Phosphorylation of Drp1 at S616 promotes mitochondrial fission, while phosphorylation at S637 inhibits it. Western blot analysis was used to determine the effect of IO on mitochondrial fission by quantifying p-Drp1 S616:S637 ratio, an indicator of mitochondrial fission. It was found that IO caused a significant increase in phosphorylation S616:S637 ratio in EV control cells, but not in the MitoN cells (Fig. 2A) indicating IO upregulated Drp1-dependent mitochondrial fission. To further assess the effects of IO on mitochondrial fission, the expression level of different Drp1 receptors was examined by western blot. Fis1 and mitochondrial fission factor are two known receptors localized to the outer mitochondrial membrane that recruit Drp1 to mediate mitochondrial fission. IO significantly increased the expression levels of Fis1 in EV cells, while the level of Fis1 remained unaffected in MitoN cells (Fig. 2B). Mitochondrial fission factor remained largely unaffected by IO in both EV and MitoN cells (Fig. 2C). Mitochondrial fusion proteins Opa1, Mfn1, and Mfn2 were largely unaffected (Fig. 2E-G). However, there was a decrease in Mfn1 upon IO in the MitoN but not EV cells (Fig. 2F). PGC1α, a critical mediator of mitochondrial biogenesis, was unaffected by IO, but MitoN itself enhanced the expression level (Fig. 2H). Mitochondrial fission was visually assessed by staining mitochondria with the fluorescent dye, Mitotracker green. Quantitative analysis of mitochondrial networks showed that IO decreased mitochondrial length and networking and increased sphericity (indicative of increased mitochondrial fission) in EV cells, but not in MitoN cells (Fig 2I, J).

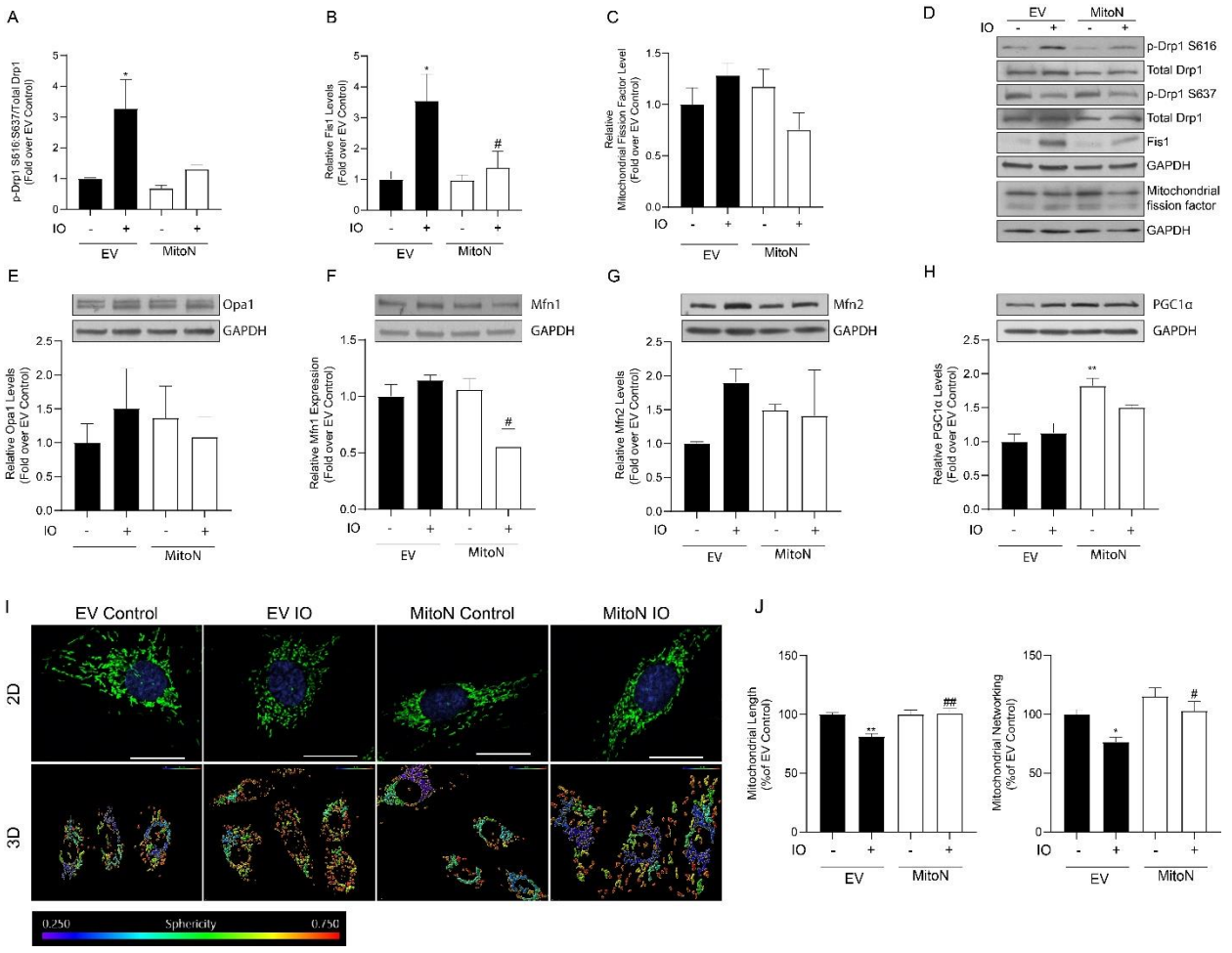

Figure 2. MitoNEET prevents IO-induced mitochondrial fragmentation. The relative level of mitochondrial fission was assessed in L6 EV and MitoN cells treated with (IO) or without (control) iron by western blot analysis of mitochondrial fission related proteins **(A)** p-Drp1, n=4; **(B)** Fis1, n=5; and **(C)** mitochondrial fission factor, n=5. **(D)** Representative blots along with loading control are shown for each fission related protein. Relative levels of mitochondrial fusion were assessed in L6 EV and MitoN cells treated with (IO) or without (control) iron for 24 hours by western blot analysis of mitochondrial fusion related proteins **(E)** Opa1, n=4; **(F)** Mfn1, n=5; and **(G)** Mfn2, n=4. Representative blots along with loading control are shown for each fusion related protein above graphs. **(H)** PGC1α in L6 EV and MitoN cells treated with (IO) or without (control) iron for 24 hours was quantified by western blot analysis, n=3. **(I)** Mitochondrial fission was visualized in 2D and 3D using Mitotracker green in L6 EV and MitoN cells treated with (IO) or without (control) iron for 24 hours. For 2D images, scalebar = 20µm. For 3D images, scalebar = 5µm. **(J)** Quantification of mitochondrial length and networking for images from I, n=4. *Indicates significant difference compared to EV control, p<0.05. **Indicates significant difference compared to EV control, p<0.01. #Indicates significant difference compared to EV IO, p<0.05. ##Indicates significant difference compared to EV IO, p<0.01.

IO-induced insulin resistance is mediated by mitochondrial ROS and fission

Mitochondrial fission is closely related to oxidative stress. To determine whether oxidative stress was pertinent to this study, mitochondrial ROS was quantified using MitoSOX staining. Upon IO, L6 EV cells exhibited an increase in mitochondrial ROS, however this was not observed in MitoN cells (Fig. 3A, B). This increase in mitochondrial

ROS was found to be linked to IO-induced mitochondrial fission. In the absence of Skq1, IO decreased mitochondrial length and networking and increased sphericity suggestive of increased fission (Fig. 3C - E). Although the use of Skq1, a mitochondrial antioxidant, showed signs of increased fission, the deleterious effects of IO were averted, indicating mitochondrial ROS and fission are linked (Fig. 3C – E). Having characterized an increase in both mitochondrial fission and ROS upon IO, the relationship to insulin resistance was subsequently explored. To determine if mitochondrial ROS and fission played a causal role in the onset of IO-induced insulin resistance, insulin signaling was measured using L6 Akt biosensor cells in the presence of the mitochondrial antioxidant, Skq1, or mitochondrial fission inhibitor, Mdivi-1. Pretreatment with both Skq1 (Fig. 3F, G) and Mdivi-1 (Fig. 3H, I) restored insulin-stimulated nuclear FOXO1 export to levels similar to that of control indicating both mitochondrial ROS and fission directly contribute to the development of IO-induced insulin resistance.

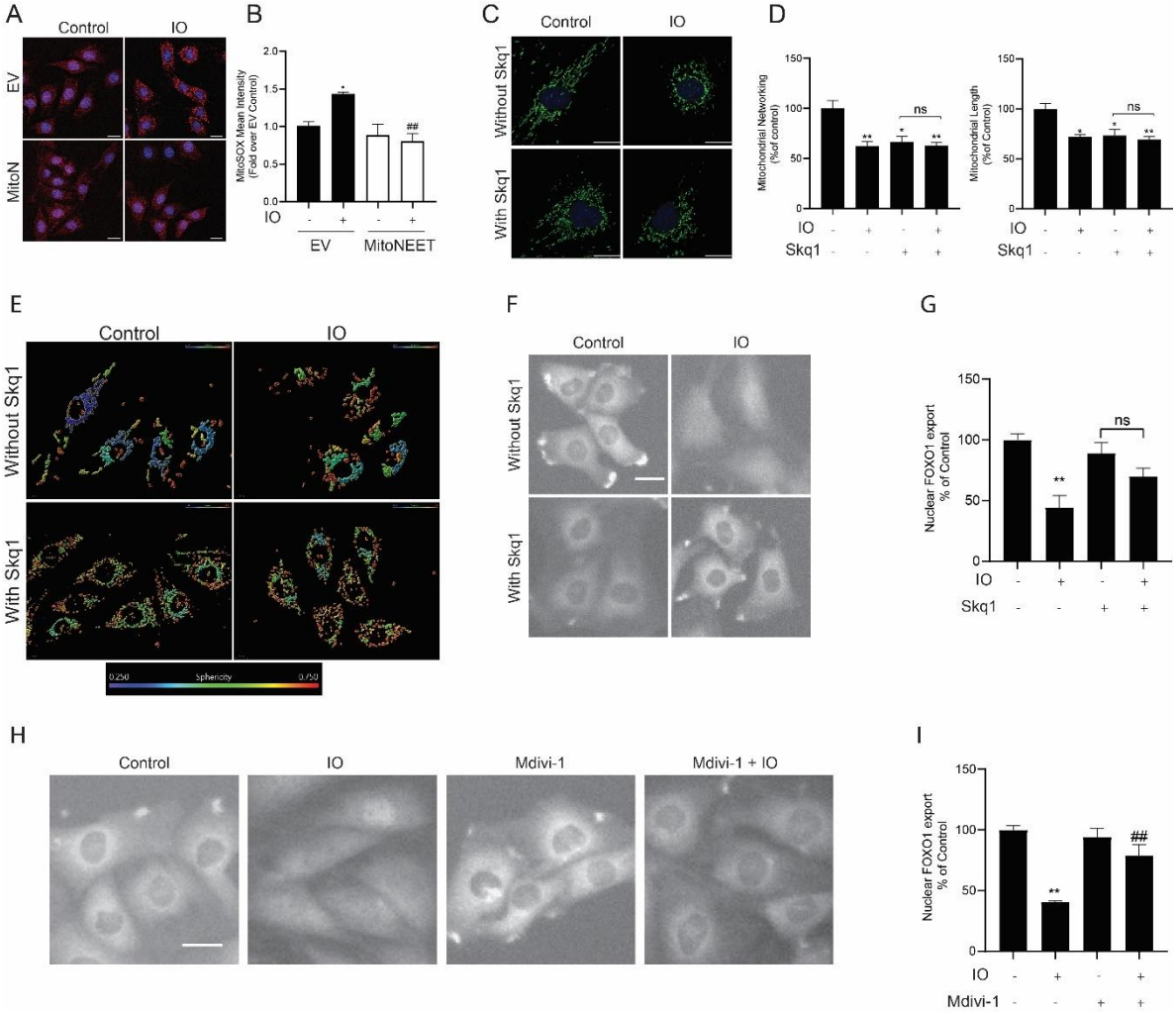

Figure 3. IO-induced insulin resistance is mediated by mitochondrial ROS and fission. **(A, B)** Assessment of mitochondrial ROS by mitoSOX staining in L6 EV and MitoN cells treated with (IO) or without (control) iron for 4 h. mitoSOX fluorescent images representative of n=3 is shown, scale bar = 20μm. **(C, D)** Visualization and analysis of mitochondrial network of L6 EV cells treated with (IO) or without (control) iron for 24 hours. Where indicated, cells were treated with 20nM Skq1 for 30 minutes prior to iron treatment. **(E)** Representative images in 3D are shown. Scale bar indicates 20μm in figure C and 10μm in figure E. **(F, G)** Assessment of insulin signaling using an Akt biosensor in L6 EV cells. Quantification of nuclear FOXO1 export along with representative images are shown, n=3. Where indicated, cells were pretreated with 20nM Skq1 for 30 minutes. Scalebar = 10μm. **(H, I)** Assessment of insulin signaling using an Akt biosensor in L6 EV cells. Quantification of nuclear FOXO1 export along with representative images are shown, n=3. Where indicated, cells were pretreated with 3μM Mdivi-1 for 30 minutes. Scalebar = 10μm *Indicates significant difference compared to EV control, $p<0.05$. **Indicates significant difference compared to EV control, $p<0.01$. #Indicates significant difference compared to EV IO, $p<0.05$.

MitoNEET downregulates mitophagy upon IO

Impaired mitophagy has been observed in models of diabetes [88]. Additionally, increased mitophagy through overexpression of mitophagy-related proteins in animal models has demonstrated some therapeutic potential against insulin resistance [40]. The role of mitoNEET in mitophagy under conditions of IO was examined.

The effect of IO on mitophagy was assessed by western blot of autophagy and mitophagy markers in mitochondrial fractions in L6 EV and MitoN cells. Upon short duration of IO (4 h), there was an increase in LC3-II in EV but decreased in MitoN (Fig. 4A). The levels of p62 were unchanged in all groups following 4 h IO (Fig. 4B). Together, this indicated that 4 h IO increased autophagosome formation in EV but decreased in MitoN. A decreased autophagosome formation upon IO in MitoN cells may indicate mitophagy initiation is impaired. Parkin is a protein that is translocated from the cytosol to the mitochondria during the initiation stage of mitophagy. Following 4hr IO, both EV and MitoN cells showed a decrease in levels of Parkin, though this did not reach statistical significance (Fig. 4C).

The effects of longer duration of IO (24 h) were assessed. Upon 24 h IO, LC3-II and p62 was increased in both L6 EV and MitoN cells (Fig. 4D,E). The levels of LC3-II and p62 in IO-treated MitoN cells were also higher than the IO-treated EV cells. Together, this indicates that's 24hr IO causes autophagosome accumulation suggestive of mitophagy impairment, which is augmented by MitoN. Levels of Parkin in both EV and MitoN were decreased upon 24hr IO which further illustrates the impairment in mitophagy upon IO (Fig 4F).

Receptor-mediated mitophagy was assessed by qPCR of BNIP3, BNIP3L, and FUNDC1. Upon 24 h IO, BNIP3 and BNIP3L increased in both EV and MitoN, however this did not reach statistical significance (Fig. 4G, H). In EV, IO also induced a >80-fold increase in FUNDC1 but remained largely unchanged in MitoN (Fig. 4I).

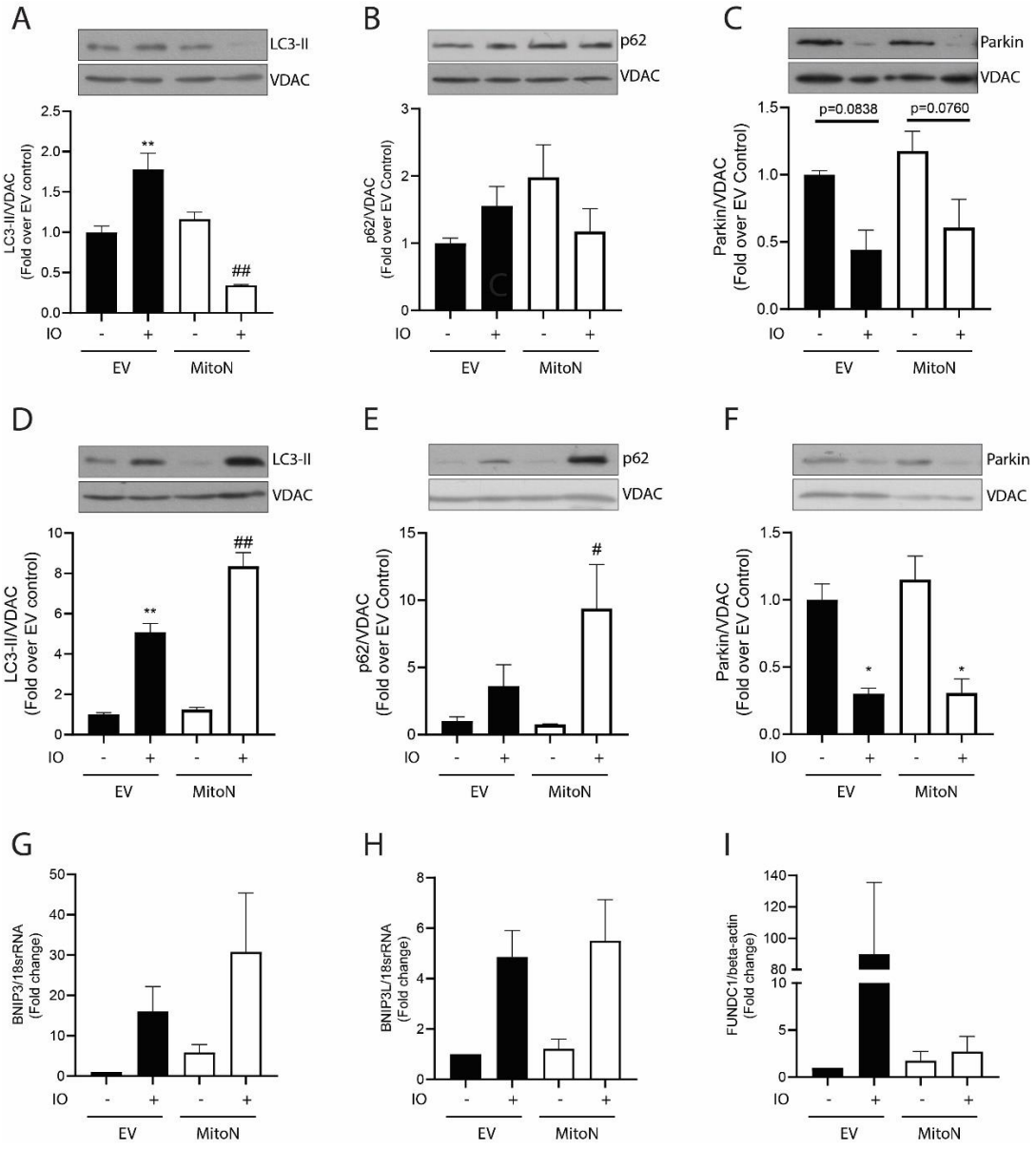

Figure 4. MitoNEET downregulates mitophagy upon IO. Assessment of mitophagy in L6 EV and MitoN cells treated with (IO) or without (control) iron for 4 h by western blot of **(A)** LC3-II (n=3), **(B)** P62 (n=5), and **(C)** Parkin (n=4) in mitochondrial fractions. Representative blots along with loading control are shown above graphs. Assessment of mitophagy in L6 EV and MitoN cells treated with (IO) or without (control) iron for 24 hours by western blot of **(E)** LC3-II, **(F)** P62, and **(G)** Parkin in mitochondrial fractions. Representative blots along with loading control are shown above graphs, n=3. (G-I) Evaluation of receptor-mediated mitophagy in L6 EV and MitoN cells treated with (IO) or without (control) iron for 24 h. Quantification of **(G)** BNIP, **(H)** BNIP3L, and **(I)** FUNDC1 gene expression are shown, n=3. *Indicates significant difference compared to EV control, $p<0.05$. **Indicates significant difference compared to EV control, $p<0.01$. #Indicates significant difference compared to EV IO, $p<0.05$. ##Indicates significant difference compared to EV IO, $p<0.01$.

3.5 Discussion

The prevalence of diabetes worldwide was 8.8% in 2015 and is projected to increase to 10.4% by 2040 [89]. A quarter of the global population is estimated to suffer from metabolic syndrome, a group of risk factors, that increases the risk of developing heart disease, stroke, and T2D [24,90]. One of the earliest hallmarks of metabolic syndrome is the presence of insulin resistance [24]. Furthermore, insulin resistance has been observed in humans up to 10 years prior to the diagnosis of T2D and the treatment of insulin resistance is regarded as an effective strategy in delaying progression to T2D [59]. Therefore, therapies aimed at insulin resistance are important in the prevention of T2D.

Here, mitochondrial iron was shown to play an important role in causing insulin resistance in L6 skeletal muscle cells, which could be regulated by MitoNEET overexpression. Using an *in vitro* model of IO, a significant amount of iron accumulated in mitochondria demonstrated by MFF staining and mitochondrial ferritin. This accumulation of mitochondrial iron was associated with increased mitochondrial ROS demonstrated using MitoSOX and increased mitochondrial fission via the Fis1 pathway as shown by western blot and visual analysis of mitochondria. Mitochondrial ROS and fission were causally linked to the development of IO-induced insulin resistance which was shown by western blot and Akt biosensor cells. Finally, it was demonstrated that IO downregulated Parkin-dependent mitophagy, but upregulated receptor-mediated mitophagy. Moreover, FUNDC1-dependent mitophagy could potentially be downregulated by mitoNEET during IO conditions.

There are several underlying causes of insulin resistance that have been established [91]. However, the important role of IO in mediating insulin resistance remains understated and incompletely understood in the literature [16]. Dysregulation of iron has been strongly correlated with metabolic syndrome and insulin resistance. For example, elevated serum ferritin, a marker of excess body iron stores, was correlated with an elevated risk of diabetes [92]. Similarly, increased ferritin levels were also correlated with high triglyceride and glucose levels [92]. Increased transferrin saturation % is another index of body iron stores which has been associated with insulin resistance and T2D [93]. For instance, 50% transferrin saturation or higher increased risk of developing T2D nearly two-fold [93]. My data further supports the idea that IO plays an important role in mediating insulin resistance. Moreover, I demonstrated the therapeutic potential of regulating mitochondrial iron via mitoNEET overexpression in the context of insulin resistance. As a result, targeting mitochondrial iron could be a potential therapeutic strategy in the treatment on insulin resistance and T2D.

Disrupted mitochondrial dynamics, specifically a shift towards fission, has been causally associated with insulin resistance [30]. The data presented here showed fission was upregulated by IO using visual analysis of fluorescent stained mitochondria and western blot analysis of fission related proteins. Two distinct pathways of fission have been identified, both of which require Drp1, but the receptor proteins involved and mitochondria fate differ [94]. Mitochondria that undergo fission via the Fis1 pathway subsequently undergo degradation, whereas mitochondria that proceed through the mitochondrial fission factor pathway ultimately undergo biogenesis [94]. Fis1-dependent fission is often proceeded by mitochondria with decreased membrane potential, and

elevated ROS suggesting signs of dysfunction [94]. In this study, IO was found to upregulate Fis1-dependent fission without altering mitochondrial fission factor-dependent fission. The elevated Fis1 indicated IO may have caused some form of mitochondrial dysfunction prior to the fission event.

Oxidative stress and mitochondrial dynamics are intricately linked, and both play a key role in the development of insulin resistance [60]. It has been widely accepted that fission events lead to increased ROS and vice versa, however, the effect of ROS on mitochondrial dynamics has been less characterized [17]. Using MitoSOX, it was shown that IO upregulated mitochondrial ROS and was prevented by MitoNEET. Further examination into the role of mitochondrial ROS using the mitochondrial antioxidant, Skq1, illustrated that IO-induced fission was dependent on mitochondrial ROS where Skq1 prevented the fission promoting effect of IO. The pharmacological inhibition of fission has been shown to have some therapeutic effect in a model of obesity-induced insulin resistance [93]. In this study, the use of fission inhibitor, Mdivi-1, or mitochondrial ROS inhibitor, Skq1, prevented IO-induced insulin resistance. Taken together, this indicates a IO causes insulin resistance through a mitochondrial ROS/fission-dependent manner.

In conclusion, mitochondrial iron is implicated in the development of skeletal muscle insulin resistance. Furthermore, the beneficial effect of regulating mitochondria iron through MitoNEET overexpression was demonstrated to prevent the deleterious effects of IO, thus averting insulin resistance. Mechanistically, IO elevated Fis1-dependent fission and mitochondrial ROS which directly cause insulin resistance. During IO, FUNDC1-dependent mitophagy was upregulated which may potentially contribute to the development of insulin resistance, though, further investigations are required.

4 Conclusions

The studies presented above defined a critical role of mitochondria-specific iron and mitochondrial ROS in the development of insulin resistance in an *in vitro* model mimicking a cardiac and skeletal muscle setting. These findings build upon previous findings and the current literature that implicate excess iron in the development of insulin resistance. Furthermore, my thesis highlighted the therapeutic potential of the mitoNEET protein in its ability to regulate mitochondrial iron and avoid subsequent insulin resistance. I also demonstrated mitoNEET to play some role in altering mitochondrial dynamics and mitophagy under iron overload conditions.

5 Future directions

Translate findings to an *in vivo* model

The *in vitro* findings from my thesis lays a solid foundation upon which to expand to an *in vivo* setting. The use of an *in vivo* system will allow for a better understanding of the role of mitoNEET in a more physiologically relevant setting. Translating these *in vitro* findings to an *in vivo* setting, can be accomplished using a mouse model with an overexpression of mitoNEET in specific tissue such as cardiac or skeletal muscle [46]. For example, transgenic mice with an inducible and tissue-specific overexpression of mitoNEET has been described in the literature [46]. The overexpression of mitoNEET in a tissue specific manner was accomplished using a tetracycline on system in combination with the Cre/LoxP system. Alternatively, the role of mitoNEET can be investigated *in vivo* using a knockout approach. In the literature, a mouse model with cardiac-specific knockout of mitoNEET has been generated using the Cre/LoxP system [95]. The

Cre/LoxP system is a tool that can be used to manipulate gene expression in a tissue-specific manner. Similar method can be applied to alter expression of mitoNEET in skeletal muscle [96,97]. Translating these findings into a more physiologically relevant system will aid in the development of improved therapeutic strategies.

Characterize the role of FUNDC1-dependent mitophagy

The literature largely suggests impairment of mitophagy is linked with insulin resistance. Based on this, activation of mitophagy has been speculated to be therapeutic for insulin resistance [40]. However, these generalizations are based primarily on studies in adipose tissues [40]. In contrast to this idea, ablation of FUNDC1 in skeletal muscle resulted in mitophagy impairment which conferred protection against high-fat diet induced insulin resistance [44]. Furthermore, the exact role of FUNDC1-dependent mitophagy under conditions of IO has not been established and requires further investigations.

To elucidate the precise role of FUNDC1 in IO-induced insulin resistance, L6 cells with FUNDC1 knockout will be generated. The insulin signaling can then be assessed by western blotting and Akt biosensor cells in the absence or presence of IO. Findings from this approach will shed light on whether FUNDC1 is protective or contributes to the development of IO-induced insulin resistance in skeletal muscle.

6 Statement of contributions

Chapter 2

Eddie Tam designed and carried out all experiments (with contributions from co-authors), wrote initial draft, and made all revisions for publication. It has been published in Journal of Cellular Physiology as of June 2023 [98]. All data pertaining to Figure 1D-F were completed in partial fulfillment of “BCHM4000 – Biochemistry Research Project” at York University.

Chapter 3

Experiments were designed, carried out, and results interpreted by Eddie Tam with contributions from collaborative work as indicated. Experiments pertaining to figure 3F – I and figure 4G – I were carried out by Khang Nguyen.

7 References

1 Gammella E, Recalcati S, Cairo G. Dual Role of ROS as Signal and Stress Agents: Iron Tips the Balance in favor of Toxic Effects. *Oxid Med Cell Longev* 2016; **2016**: 8629024.

2 Geldenhuys WJ, Benkovic SA, Lin L, Yonutas HM, Crish SD, Sullivan PG, Darvesh AS, Brown CM, Richardson JR. MitoNEET (CISD1) Knockout Mice Show Signs of Striatal Mitochondrial Dysfunction and a Parkinson's Disease Phenotype. *ACS Chem Neurosci* 2017; **8**: 2759–65.

3 Paul BT, Manz DH, Torti FM, Torti SV. Mitochondria and Iron: current questions. *Expert Rev Hematol* 2017; **10**: 65–79.

4 Pantopoulos K, Porwal SK, Tartakoff A, Devireddy L. Mechanisms of mammalian iron homeostasis. *Biochemistry* 2012; **51**: 5705–24.

5 Theil EC. Ferritin: the protein nanocage and iron biomineral in health and in disease. *Inorg Chem* 2013; **52**: 12223–33.

6 Wilkinson N, Pantopoulos K. The IRP/IRE system in vivo: insights from mouse models. *Front Pharmacol* 2014; **5**: 176.

7 Gammella E, Recalcati S, Rybinska I, Buratti P, Cairo G. Iron-induced damage in cardiomyopathy: oxidative-dependent and independent mechanisms. *Oxid Med Cell Longev* 2015; **2015**: 230182.

8 Pitchika A, Schipf S, Nauck M, Dörr M, Lerch MM, Felix SB, Markus MRP, Völzke H, Ittermann T. Associations of iron markers with type 2 diabetes mellitus and metabolic syndrome: Results from the prospective SHIP study. *Diabetes Res Clin Pract* 2020; **163**: 108149.

9 Wang W, Knovich MA, Coffman LG, Torti FM, Torti SV. Serum Ferritin: Past, Present and Future. *Biochim Biophys Acta* 2010; **1800**: 760–9.

10 Gattermann N, Muckenthaler MU, Kulozik AE, Metzgeroth G, Hastka J. The Evaluation of Iron Deficiency and Iron Overload. *Dtsch Arztebl Int* 2021; **118**: 847–56.

11 Kratz A, Ferraro M, Sluss PM, Lewandrowski KB. Case records of the Massachusetts General Hospital. Weekly clinicopathological exercises. Laboratory reference values. *N Engl J Med* 2004; **351**: 1548–63.

12 Knovich MA, Storey JA, Coffman LG, Torti SV, Torti FM. Ferritin for the clinician. *Blood Rev* 2009; **23**: 95–104.

13 Hoffman R, Benz EJ, Silberstein LE, Heslop HE, Weitz JI, Salama ME, Abutalib SA, editors. Hematology: basic principles and practice. Eighth edition. Philadelphia, PA: Elsevier; 2023.

14 Shannon MW, Borron SW, Burns MJ, Haddad LM, Winchester JF, editors. Haddad and Winchester's clinical management of poisoning and drug overdose. 4th ed. Philadelphia: Saunders/Elsevier; 2007.

15 Collins JF, Wessling-Resnick M, Knutson MD. Hepcidin regulation of iron transport. *J Nutr* 2008; **138**: 2284–8.

16 Simcox JA, McClain DA. Iron and diabetes risk. *Cell Metab* 2013; **17**: 329–41.

17 Ježek J, Cooper KF, Strich R. Reactive Oxygen Species and Mitochondrial Dynamics: The Yin and Yang of Mitochondrial Dysfunction and Cancer Progression. *Antioxidants (Basel)* 2018; **7**: E13.

18 Wang Z, Fang S, Ding S, Tan Q, Zhang X. Research Progress on Relationship Between Iron Overload and Lower Limb Arterial Disease in Type 2 Diabetes Mellitus. *Diabetes Metab Syndr Obes* 2022; **15**: 2259–64.

19 Phaniendra A, Jestadi DB, Periyasamy L. Free radicals: properties, sources, targets, and their implication in various diseases. *Indian J Clin Biochem* 2015; **30**: 11–26.

20 Boucher J, Kleinridders A, Kahn CR. Insulin receptor signaling in normal and insulin-resistant states. *Cold Spring Harb Perspect Biol* 2014; **6**: a009191.

21 Garvey WT, Ryan DH, Henry R, Bohannon NJV, Toplak H, Schwiers M, Troupin B, Day WW. Prevention of type 2 diabetes in subjects with prediabetes and metabolic syndrome treated with phentermine and topiramate extended release. *Diabetes Care* 2014; **37**: 912–21.

22 Alberti KGMM, Eckel RH, Grundy SM, Zimmet PZ, Cleeman JI, Donato KA, Fruchart J-C, James WPT, Loria CM, Smith SC, International Diabetes Federation Task Force on Epidemiology and Prevention, Hational Heart, Lung, and Blood Institute, American Heart Association, World Heart Federation, International Atherosclerosis Society, International Association for the Study of Obesity. Harmonizing the metabolic syndrome: a joint interim statement of the International Diabetes Federation Task Force on Epidemiology and Prevention; National Heart, Lung, and Blood Institute; American Heart Association; World Heart Federation; International Atherosclerosis Society; and International Association for the Study of Obesity. *Circulation* 2009; **120**: 1640–5.

23 Eckel RH, Grundy SM, Zimmet PZ. The metabolic syndrome. *Lancet* 2005; **365**: 1415–28.

24 Saklayen MG. The Global Epidemic of the Metabolic Syndrome. *Curr Hypertens Rep* 2018; **20**: 12.

25 Kelishadi R. Metabolic syndrome burden in children and adolescents. *Lancet Child Adolesc Health* 2022; **6**: 138–9.

26 Bozzini C, Girelli D, Olivieri O, Martinelli N, Bassi A, De Matteis G, Tenuti I, Lotto V, Friso S, Pizzolo F, Corrocher R. Prevalence of body iron excess in the metabolic syndrome. *Diabetes Care* 2005; **28**: 2061–3.

27 Rametta R, Fracanzani AL, Fargion S, Dongiovanni P. Dysmetabolic Hyperferritinemia and Dysmetabolic Iron Overload Syndrome (DIOS): Two Related Conditions or Different Entities? *Curr Pharm Des* 2020; **26**: 1025–35.

28 Alberti KGMM, Zimmet P, Shaw J. Metabolic syndrome--a new world-wide definition. A Consensus Statement from the International Diabetes Federation. *Diabet Med* 2006; **23**: 469–80.

29 Murphy MP, Hartley RC. Mitochondria as a therapeutic target for common pathologies. *Nat Rev Drug Discov* 2018; **17**: 865–86.

30 Jheng H-F, Tsai P-J, Guo S-M, Kuo L-H, Chang C-S, Su I-J, Chang C-R, Tsai Y-S. Mitochondrial fission contributes to mitochondrial dysfunction and insulin resistance in skeletal muscle. *Mol Cell Biol* 2012; **32**: 309–19.

31 Sebastián D, Hernández-Alvarez MI, Segalés J, Sorianello E, Muñoz JP, Sala D, Waget A, Liesa M, Paz JC, Gopalacharyulu P, Orešič M, Pich S, Burcelin R, Palacín M, Zorzano A. Mitofusin 2 (Mfn2) links mitochondrial and endoplasmic reticulum function with insulin signaling and is essential for normal glucose homeostasis. *Proc Natl Acad Sci U S A* 2012; **109**: 5523–8.

32 Sergi D, Naumovski N, Heilbronn LK, Abeywardena M, O'Callaghan N, Lionetti L, Luscombe-Marsh N. Mitochondrial (Dys)function and Insulin Resistance: From Pathophysiological Molecular Mechanisms to the Impact of Diet. *Front Physiol* 2019; **10**: 532.

33 Youle RJ, van der Bliek AM. Mitochondrial fission, fusion, and stress. *Science* 2012; **337**: 1062–5.

34 Ohsumi Y. Historical landmarks of autophagy research. *Cell Res* 2014; **24**: 9–23.

35 Hurley JH, Young LN. Mechanisms of Autophagy Initiation. *Annu Rev Biochem* 2017; **86**: 225–44.

36 Klionsky DJ, Abdel-Aziz AK, Abdelfatah S, Abdellatif M, Abdoli A, Abel S, Abeliovich H, Abildgaard MH, Abudu YP, Acevedo-Arozena A, Adamopoulos IE, Adeli K, Adolph TE, Adornetto A, Aflaki E, Agam G, Agarwal A, Aggarwal BB, Agnello M, Agostinis P, et al. Guidelines for the use and interpretation of assays for monitoring autophagy (4th edition)1. *Autophagy* 2021; **17**: 1–382.

37 Parzych KR, Klionsky DJ. An overview of autophagy: morphology, mechanism, and regulation. *Antioxid Redox Signal* 2014; **20**: 460–73.

38 Jahng JWS, Alsaadi RM, Palanivel R, Song E, Hipolito VEB, Sung HK, Botelho RJ, Russell RC, Sweeney G. Iron overload inhibits late stage autophagic flux leading to insulin resistance. *EMBO Rep* 2019; **20**: e47911.

39 Sung HK, Song E, Jahng JWS, Pantopoulos K, Sweeney G. Iron induces insulin resistance in cardiomyocytes via regulation of oxidative stress. *Sci Rep* 2019; **9**: 4668.

40 Ning P, Jiang X, Yang J, Zhang J, Yang F, Cao H. Mitophagy: A potential therapeutic target for insulin resistance. *Front Physiol* 2022; **13**: 957968.

41 Jin SM, Youle RJ. PINK1- and Parkin-mediated mitophagy at a glance. *J Cell Sci* 2012; **125**: 795–9.

42 Li Y, Zheng W, Lu Y, Zheng Y, Pan L, Wu X, Yuan Y, Shen Z, Ma S, Zhang X, Wu J, Chen Z, Zhang X. BNIP3L/NIX-mediated mitophagy: molecular mechanisms and implications for human disease. *Cell Death Dis* 2021; **13**: 14.

43 Liu L, Feng D, Chen G, Chen M, Zheng Q, Song P, Ma Q, Zhu C, Wang R, Qi W, Huang L, Xue P, Li B, Wang X, Jin H, Wang J, Yang F, Liu P, Zhu Y, Sui S, et al. Mitochondrial outer-membrane protein FUNDC1 mediates hypoxia-induced mitophagy in mammalian cells. *Nat Cell Biol* 2012; **14**: 177–85.

44 Fu T, Xu Z, Liu L, Guo Q, Wu H, Liang X, Zhou D, Xiao L, Liu L, Liu Y, Zhu M-S, Chen Q, Gan Z. Mitophagy Directs Muscle-Adipose Crosstalk to Alleviate Dietary Obesity. *Cell Rep* 2018; **23**: 1357–72.

45 Colca JR, McDonald WG, Waldon DJ, Leone JW, Lull JM, Bannow CA, Lund ET, Mathews WR. Identification of a novel mitochondrial protein (“mitoNEET”) cross-linked specifically by a thiazolidinedione photoprobe. *Am J Physiol Endocrinol Metab* 2004; **286**: E252-260.

46 Kusminski CM, Holland WL, Sun K, Park J, Spurgin SB, Lin Y, Askew GR, Simcox JA, McClain DA, Li C, Scherer PE. MitoNEET-driven alterations in adipocyte mitochondrial activity reveal a crucial adaptive process that preserves insulin sensitivity in obesity. *Nat Med* 2012; **18**: 1539–49.

47 Geldenhuys WJ, Leeper TC, Carroll RT. mitoNEET as a novel drug target for mitochondrial dysfunction. *Drug Discov Today* 2014; **19**: 1601–6.

48 Wiley SE, Murphy AN, Ross SA, van der Geer P, Dixon JE. MitoNEET is an iron-containing outer mitochondrial membrane protein that regulates oxidative capacity. *Proc Natl Acad Sci U S A* 2007; **104**: 5318–23.

49 Chen X-Y, Ren H-H, Wang D, Chen Y, Qu C-J, Pan Z-H, Liu X-N, Hao W-J, Xu W-J, Wang K-J, Li D-F, Zheng Q-S. Isoliquiritigenin Induces Mitochondrial Dysfunction and Apoptosis by Inhibiting mitoNEET in a Reactive Oxygen Species-Dependent Manner in A375 Human Melanoma Cells. *Oxid Med Cell Longev* 2019; **2019**: 9817576.

50 Habener A, Chowdhury A, Echtermeyer F, Lichtinghagen R, Theilmeier G, Herzog C. MitoNEET Protects HL-1 Cardiomyocytes from Oxidative Stress Mediated Apoptosis in an In Vitro Model of Hypoxia and Reoxygenation. *PLoS One* 2016; **11**: e0156054.

51 Zuris JA, Ali SS, Yeh H, Nguyen TA, Nechushtai R, Paddock ML, Jennings PA. NADPH inhibits [2Fe-2S] cluster protein transfer from diabetes drug target MitoNEET to an apo-acceptor protein. *J Biol Chem* 2012; **287**: 11649–55.

52 Guariguata L, Whiting DR, Hambleton I, Beagley J, Linnenkamp U, Shaw JE. Global estimates of diabetes prevalence for 2013 and projections for 2035. *Diabetes Res Clin Pract* 2014; **103**: 137–49.

53 Kharroubi AT, Darwish HM. Diabetes mellitus: The epidemic of the century. *World J Diabetes* 2015; **6**: 850–67.

54 Miki T, Yuda S, Kouzu H, Miura T. Diabetic cardiomyopathy: pathophysiology and clinical features. *Heart Fail Rev* 2013; **18**: 149–66.

55 Sun L, Yu M, Zhou T, Zhang S, He G, Wang G, Gang X. Current advances in the study of diabetic cardiomyopathy: From clinicopathological features to molecular therapeutics (Review). *Mol Med Rep* 2019; **20**: 2051–62.

56 Tam E, Sung HK, Lam NH, You S, Cho S, Ahmed SM, Abdul-Sater AA, Sweeney G. Role of Mitochondrial Iron Overload in Mediating Cell Death in H9c2 Cells. *Cells* 2022; **12**: 118.

57 Kholmukhamedov A, Li L, Lindsey CC, Hu J, Nieminen A-L, Takemoto K, Beeson GC, Beneker CM, McInnes C, Beeson CC, Lemasters JJ. A new fluorescent sensor mitoferrofluor indicates the presence of chelatable iron in polarized and depolarized mitochondria. *J Biol Chem* 2022; **298**: 102336.

58 Valente AJ, Maddalena LA, Robb EL, Moradi F, Stuart JA. A simple ImageJ macro tool for analyzing mitochondrial network morphology in mammalian cell culture. *Acta Histochem* 2017; **119**: 315–26.

59 Hulman A, Simmons RK, Brunner EJ, Witte DR, Færch K, Vistisen D, Ikehara S, Kivimaki M, Tabák AG. Trajectories of glycaemia, insulin sensitivity and insulin secretion in South Asian and white individuals before diagnosis of type 2 diabetes: a longitudinal analysis from the Whitehall II cohort study. *Diabetologia* 2017; **60**: 1252–60.

60 Hurrle S, Hsu WH. The etiology of oxidative stress in insulin resistance. *Biomed J* 2017; **40**: 257–62.

61 Bjelakovic G, Nikolova D, Gluud LL, Simonetti RG, Gluud C. Mortality in randomized trials of antioxidant supplements for primary and secondary prevention: systematic review and meta-analysis. *JAMA* 2007; **297**: 842–57.

62 Vivekananthan DP, Penn MS, Sapp SK, Hsu A, Topol EJ. Use of antioxidant vitamins for the prevention of cardiovascular disease: meta-analysis of randomised trials. *Lancet* 2003; **361**: 2017–23.

63 Chen L, Gong Q, Stice JP, Knowlton AA. Mitochondrial OPA1, apoptosis, and heart failure. *Cardiovasc Res* 2009; **84**: 91–9.

64 Kelley DE, He J, Menshikova EV, Ritov VB. Dysfunction of mitochondria in human skeletal muscle in type 2 diabetes. *Diabetes* 2002; **51**: 2944–50.

65 Abbaspour N, Hurrell R, Kelishadi R. Review on iron and its importance for human health. *J Res Med Sci* 2014; **19**: 164–74.

66 Liu J, Li Q, Yang Y, Ma L. Iron metabolism and type 2 diabetes mellitus: A meta-analysis and systematic review. *J Diabetes Investig* 2020; **11**: 946–55.

67 Cooksey RC, Jones D, Gabrielsen S, Huang J, Simcox JA, Luo B, Soesanto Y, Rienhoff H, Abel ED, McClain DA. Dietary iron restriction or iron chelation protects from diabetes and loss of beta-cell function in the obese (ob/ob lep-/-) mouse. *Am J Physiol Endocrinol Metab* 2010; **298**: E1236-1243.

68 Mobarra N, Shanaki M, Ehteram H, Nasiri H, Sahmani M, Saeidi M, Goudarzi M, Pourkarim H, Azad M. A Review on Iron Chelators in Treatment of Iron Overload Syndromes. *Int J Hematol Oncol Stem Cell Res* 2016; **10**: 239–47.

69 Mamtani M, Kulkarni H. Influence of iron chelators on myocardial iron and cardiac function in transfusion-dependent thalassaemia: a systematic review and meta-analysis. *Br J Haematol* 2008; **141**: 882–90.

70 Ma Y, Abbate V, Hider RC. Iron-sensitive fluorescent probes: monitoring intracellular iron pools. *Metallomics* 2015; **7**: 212–22.

71 Fakih S, Podinovskaia M, Kong X, Collins HL, Schaible UE, Hider RC. Targeting the lysosome: fluorescent iron(III) chelators to selectively monitor endosomal/lysosomal labile iron pools. *J Med Chem* 2008; **51**: 4539–52.

72 Sohn Y-S, Breuer W, Munnich A, Cabantchik ZI. Redistribution of accumulated cell iron: a modality of chelation with therapeutic implications. *Blood* 2008; **111**: 1690–9.

73 Peña-Montes DJ, Huerta-Cervantes M, Ríos-Silva M, Trujillo X, Cortés-Rojo C, Huerta M, Saavedra-Molina A. Effects of dietary iron restriction on kidney

mitochondria function and oxidative stress in streptozotocin-diabetic rats. *Mitochondrion* 2020; **54**: 41–8.

74 Shaw GC, Cope JJ, Li L, Corson K, Hersey C, Ackermann GE, Gwynn B, Lambert AJ, Wingert RA, Traver D, Trede NS, Barut BA, Zhou Y, Minet E, Donovan A, Brownlie A, Balzan R, Weiss MJ, Peters LL, Kaplan J, et al. Mitoferrin is essential for erythroid iron assimilation. *Nature* 2006; **440**: 96–100.

75 Brand MD, Orr AL, Perevoshchikova IV, Quinlan CL. The role of mitochondrial function and cellular bioenergetics in ageing and disease. *Br J Dermatol* 2013; **169 Suppl 2**: 1–8.

76 Palmer CS, Osellame LD, Laine D, Koutsopoulos OS, Frazier AE, Ryan MT. MiD49 and MiD51, new components of the mitochondrial fission machinery. *EMBO Rep* 2011; **12**: 565–73.

77 Kim J-A, Wei Y, Sowers JR. Role of mitochondrial dysfunction in insulin resistance. *Circ Res* 2008; **102**: 401–14.

78 Murphy MP. How mitochondria produce reactive oxygen species. *Biochem J* 2009; **417**: 1–13.

79 Zhao R-Z, Jiang S, Zhang L, Yu Z-B. Mitochondrial electron transport chain, ROS generation and uncoupling (Review). *Int J Mol Med* 2019; **44**: 3–15.

80 Sangwung P, Petersen KF, Shulman GI, Knowles JW. Mitochondrial Dysfunction, Insulin Resistance, and Potential Genetic Implications. *Endocrinology* 2020; **161**: bqaa017.

81 Lin H-Y, Weng S-W, Chang Y-H, Su Y-J, Chang C-M, Tsai C-J, Shen F-C, Chuang J-H, Lin T-K, Liou C-W, Lin C-Y, Wang P-W. The Causal Role of Mitochondrial Dynamics in Regulating Insulin Resistance in Diabetes: Link through Mitochondrial Reactive Oxygen Species. *Oxid Med Cell Longev* 2018; **2018**: 7514383.

82 Morino K, Petersen KF, Dufour S, Befroy D, Frattini J, Shatzkes N, Neschen S, White MF, Bilz S, Sono S, Pypaert M, Shulman GI. Reduced mitochondrial density and increased IRS-1 serine phosphorylation in muscle of insulin-resistant offspring of type 2 diabetic parents. *J Clin Invest* 2005; **115**: 3587–93.

83 Ritov VB, Menshikova EV, He J, Ferrell RE, Goodpaster BH, Kelley DE. Deficiency of subsarcolemmal mitochondria in obesity and type 2 diabetes. *Diabetes* 2005; **54**: 8–14.

84 Zorzano A, Liesa M, Palacín M. Mitochondrial dynamics as a bridge between mitochondrial dysfunction and insulin resistance. *Arch Physiol Biochem* 2009; **115**: 1–12.

85 Zuris JA, Harir Y, Conlan AR, Shvartsman M, Michaeli D, Tamir S, Paddock ML, Onuchic JN, Mittler R, Cabantchik ZI, Jennings PA, Nechushtai R. Facile transfer of [2Fe-2S] clusters from the diabetes drug target mitoNEET to an apo-acceptor protein. *Proc Natl Acad Sci U S A* 2011; **108**: 13047–52.

86 Vernay A, Marchetti A, Sabra A, Jauslin TN, Rosselin M, Scherer PE, Demaurex N, Orci L, Cosson P. MitoNEET-dependent formation of intermitochondrial junctions. *Proc Natl Acad Sci U S A* 2017; **114**: 8277–82.

87 Sung HK, Mitchell PL, Gross S, Marette A, Sweeney G. ALY688 elicits adiponectin-mimetic signaling and improves insulin action in skeletal muscle cells. *Am J Physiol Cell Physiol* 2022; **322**: C151–63.

88 Shan Z, Fa WH, Tian CR, Yuan CS, Jie N. Mitophagy and mitochondrial dynamics in type 2 diabetes mellitus treatment. *Aging (Albany NY)* 2022; **14**: 2902–19.

89 Ogurtsova K, da Rocha Fernandes JD, Huang Y, Linnenkamp U, Guariguata L, Cho NH, Cavan D, Shaw JE, Makaroff LE. IDF Diabetes Atlas: Global estimates for the prevalence of diabetes for 2015 and 2040. *Diabetes Res Clin Pract* 2017; **128**: 40–50.

90 Ford ES. Prevalence of the metabolic syndrome defined by the International Diabetes Federation among adults in the U.S. *Diabetes Care* 2005; **28**: 2745–9.

91 Yaribeygi H, Farrokhi FR, Butler AE, Sahebkar A. Insulin resistance: Review of the underlying molecular mechanisms. *J Cell Physiol* 2019; **234**: 8152–61.

92 Ford ES, Cogswell ME. Diabetes and serum ferritin concentration among U.S. adults. *Diabetes Care* 1999; **22**: 1978–83.

93 Ellervik C, Mandrup-Poulsen T, Andersen HU, Tybjærg-Hansen A, Frandsen M, Birgens H, Nordestgaard BG. Elevated transferrin saturation and risk of diabetes: three population-based studies. *Diabetes Care* 2011; **34**: 2256–8.

94 Kleele T, Rey T, Winter J, Zaganelli S, Mahecic D, Perreten Lambert H, Ruberto FP, Nemir M, Wai T, Pedrazzini T, Manley S. Distinct fission signatures predict mitochondrial degradation or biogenesis. *Nature* 2021; **593**: 435–9.

95 Furihata T, Takada S, Kakutani N, Maekawa S, Tsuda M, Matsumoto J, Mizushima W, Fukushima A, Yokota T, Enzan N, Matsushima S, Handa H, Fumoto Y, Nio-Kobayashi J, Iwanaga T, Tanaka S, Tsutsui H, Sabe H, Kinugawa S. Cardiac-specific loss of mitoNEET expression is linked with age-related heart failure. *Commun Biol* 2021; **4**: 138.

96 McCarthy JJ, Srikuea R, Kirby TJ, Peterson CA, Esser KA. Inducible Cre transgenic mouse strain for skeletal muscle-specific gene targeting. *Skelet Muscle* 2012; **2**: 8.

97 Yeo D, Kang C, Ji LL. PGC-1α Overexpression via Local In Vivo Transfection in Mouse Skeletal Muscle. *Methods Mol Biol* 2019; **1966**: 151–61.

98 Tam E, Sung HK, Sweeney G. MitoNEET prevents iron overload-induced insulin resistance in H9c2 cells through regulation of mitochondrial iron. *Journal Cellular Physiology* 2023; : jcp.31044.